Amplification of KCNMA1: A Potential Therapeutic Target in Prostate Cancer

Inauguraldissertation

zur

Erlangung der Würde eines Doktors der Philosophie

vorgelegt der

Philosophisch-Naturwissenschaftlichen Fakultät

der Universität Basel

von

Michael Bloch

aus Zürich

Genehmigt von der Philosophisch-Naturwissenschaftlichen Fakultät

Auf Antrag von

Prof. Dr.med. Christoph Moroni

Prof. Dr. Nancy Hynes

Prof. Dr.med. Lukas Bubendorf

Basel den 4.4.2006

Prof. Dr. sc. techn. Hans-Jakob Wirz

Summary

Prostate cancer is the most common cancer in males and the second leading cause of cancer deaths in western countries. Although most prostate cancers initially respond well to androgen withdrawal, they become inevitably resistant to this treatment and progress to hormone-insensitive disease after only a few months or years. The therapeutic options in these advanced tumors are very limited. The molecular mechanisms of how prostate cancers escape hormonal treatment are poorly understood. Identification of genetic alterations including amplifications could elucidate genes with oncogenic properties to be used as new therapeutic targets in this deadly disease. Here, we investigated amplification at 10q22 that prevails in 10-15% of hormone-insensitive prostate cancers and in the hormone-insensitive prostate cancer cell line PC-3. A core region 7 Mb of the amplicon was chosen for detailed analysis. The amplification profile of this region was unexpectedly flat and did not allow us to narrow down the region of interest or select a candidate gene based its location within the amplicon.

A number of potentially interesting genes within the amplified region based on the established or presumed biologic functions were tested for amplification and mRNA expression status in the prostate cell lines. The calcium-activated large-conductance potassium channel (KCNMA1) was chosen for detailed analysis as it showed the most consistent association between amplification and overexpression. It was highly expressed in the prostate cancer cell line with KCNMA1 amplification (PC-3) as compared to the non-amplified cell lines LNCaP, CWR22R, and BPH-1. Other interesting candidates that are amplified at 10q22 include PLAU, VDAC2, PSAP, CAMK2G, and PPP3CB. First, we ascertained that KCNMA1 amplification prevailed also in vivo using fluorescence in situ hybridization (FISH) with a probe specific for KCNMA1. Amplification was found in 16% of 119 late-stage human prostate cancers but not in 33 benign controls, 32 precursor lesions and in 105 clinically organ-confined prostate cancers on a prostate tissue microarray.

Modulation of the BK channel activity in vitro revealed that BK channel promotes growth of prostate cancer cell lines. In more detail, specific inhibition of BK channel in PC-3 by iberiotoxin reduced growth of this cell line but had no significant effect on BPH-1and LNCaP. This effect was even much more pronounced by RNA interference as shown in PC-3. This growth inhibition by RNA interference was paralleled by changes of cell size and shape, suggesting that BK channel may be involved in the regulation of cell volume. Interestingly, estradiol enhanced the growth of BPH-1 and LNCaP, but did not affect the growth of PC-3. The effect of estradiol on LNCaP and BPH-1 was prevented by iberiotoxin. This finding suggests that estradiol mediates the effect of estradiol on the growth of prostate cells that do not overexpress BK channel.

Taken together, our data suggest that the BK channel system is involved in the regulation of growth of prostate cancer cell lines and putatively also in the progression of prostate cancer in vivo. This makes KCNMA1 a potential therapeutic target in patients with prostate cancers that harbor KCNMA1 amplification. However, further studies are needed to investigate KCNMA1 in human prostate cancer, as we found no significant association between gene dosage and expression in a preliminary series of fresh-frozen specimens from hormone-insensitive local recurrences. Similarly, the precise mechanisms by which KCNMA1 contributes to growth regulation remain to be elucidated.

Acknowledgements

I thank Prof. Dr. Lukas Bubendorf for the opportunity and the challenge to do this thesis.

I thank Prof. Dr. Christoph Moroni and Prof. Dr. Nancy Hynes the members of my thesis committee for supervision, critical discussion and scientific advice.

I thank Prof. Dr. Karl Kunzelmann, PD Dr. Ronald Simon, PD Dr. Peter Schraml, Dr. Kirsten Struckmann, Alex Rufle, Hedvika Novotny, and Martina Mirlacher for critical discussion and technical advice.

I thank Dr. Martin Oeggerli and Christian Ruiz for their patience.

I thank the staff of the Institute of Pathology for providing an inspiring atmosphere for daily work.

1. Introduction

1.1. Epidemiology of prostate cancer

Prostate cancer is the most frequent cancer and the second leading cause of cancer related death in male [1]. The risk to be diagnosed with this cancer is very low in men below 50 years of age but greatly increases with advancing age. This strong association with age suggests changes in the aging male organism that favour development of prostate cancer. Importantly, only a small fraction of histologically detectable prostate cancers cause clinical symptoms during the patient's lieftime. The lifetime risk of 8% to be diagnosed prostate cancer contrast with the high autopsy based prevalence of up to 80% by the age of 80[2-4]. Thus, most men die with prostate cancer rather than from prostate cancer [5,6].

Widespread PSA screening for early stage prostate cancer during the past two decades has lead to a dramatic increase in the number of patients diagnosed with prostate cancer [7,8]. Potential overtreatmant of patients with PSA detected prostate cancer has become a major clinical concern [7,8]. Epidemiology suggests a genetic predisposition for prostate cancer, although no classical familial prostate cancer syndrome is known [9-11]. There is also a large racial difference in prostate cancer incidence. Afro-American men have a significantly increased risk for prostate cancer as compared to white (Caucasian) Americans. In turn, Caucasian Americans have a significantly increased risk compared to Americans of Japanese origin [12]. This might be due to different live stile especially including dietary habits [13,14]. Especially the consumption of high amount of fat is suggested to be a risk factor for prostate cancer. In contrast, regular intake of lycopenes from tomatoes is considered as a protective factor [15].

1.2. Prostate cancer development and progression

1.2.1. Benign prostate

Normal prostate glands are composed of three major cell types. Secretory luminal cells that express PSA and cytokeratins 8 and 18 [16-19]. Basal cells mediate attachment to the stroma and express high molecular weight cytokeratins. The third phenotype shows neuroendocrine differentiation and expresses chromogranins and neurosecretory products that may have growth promoting functions. Most likely, these cell types share a common origin from pluripotent stem cells located in the basal cell layer [18,20-23]. In healthy prostate the proliferation compartment is located in the basal cell layer[24]. In addition, there is a minor pool of dividing cells identified in secretory luminal cells.

Cellular diversity of the prostatic epithelium is maintained by a combination of hormonal control, growth factors and adhesive interaction with the underlying basal membrane. Secretory luminal cells are androgen dependent, and require circulating androgens for their maintenance and maturation. These cells express high levels of nuclear androgen receptor [18]. The basal cell compartment is not androgen dependent but remains androgen responsive. Subsets of these cells express androgen receptor at high levels[18]. Likely, these cells are committed to differentiate towards secretory luminal cells under appropriate androgen stimulation [25,26]. One model predicts that differentiation of prostatic epithelium is controlled by a balance of estrogen to androgen levels[27]. The prostate contains estrogen receptor α (ERα) and β (ERβ). ERβ is expressed in the majority of normal prostate epithelial cells, while ERα is typically expressed in the stromal cells and in a fraction of basal cells [27]. The physiological function of these receptors is not known. Estrogen treatment leads to atrophy of luminal cells but induces basal cell hyperplasia by preventing basal cells from differentiation towards luminal cells [25,26]. In contrast, prolonged androgen deprivation causes enhanced proliferative activity of benign luminal cells, but not of basal cells [28]. Given the well known

proproliferative function of androgens in prostate cancer it appears paradoxical that the incidence of prostate cancer increases as the androgen levels gradually decrease with age. It has been hypothesized that an imbalance between estrogens and androgens with a relative increase of estrogens upon aging may promote prostate cancer development [27].

Benign Prostatic Hyperplasia (BPH) is common in male and represents a clinically significant cause of bladder outflow obstruction in up to 40% of men during their life time [29]. However, BPH is not considered a PCa precursor. BPH occurs in the transitional zone of the prostate, whereas most clinical PCa are located in the peripheral zone of the prostate [30].

1.2.2. Prostatic intraepithelial neoplasia (PIN)

High grade PIN (HGPIN) is considered the most likely precursor of peripheral zone prostate cancer based on several pieces of evidence[31]. In autopsy series, the increase in the prevalence of PIN has been shown to precede the increasing prevalence of invasive prostate cancer by 10-15 years [16]. In addition, prostates with carcinoma have a higher amount of PIN than prostates without carcinoma. In prostate biopsies, the presence of isolated PIN is associated with an increased likelyhood of invasive prostate cancer at another site within the prostate [32]. Also, molecular profiles of PIN resemble those of prostate cancer rather than those of benign prostate[32,33].

1.2.3. Prostate cancer (PCa)

Microscopically, most carcinomas of the prostate are classical adenocarcinomas, being made up of epithelial cells with variably developed glandular architecture. During carcinogenesis the glandular structure is gradually lost. Pathological grading of the glandular organisation is basis of the Gleason grading system [34]. Gleason grading is a strong prognosticator in prostate cancer.

1.2.4. Routes of metastasis

Lymphatic or hematogeneous metastases have been found in 40% of men with PCa at the time of autopsy. Bone is most commonly involved in metatasizing PCa (90%), followed by lung (46%), liver (25%), pleura (21%), and adrenals (13%) [35]. Most bone metastases prevail in the lower spine (90% of cases of bone metastases) while other bones such as ribs (18%), long bones (15%), and skull (8%) are less commonly affected.

This metastatic pattern strongly suggests that distant spread of prostate cancer follows two different paths. A first metastatic pathway is a backward metastatic spread to the lower spine due to anastomosis between the periprostatic and the paravertebral venous plexus. A second pathway is a cava-type metastasis to lung, and from there to other organs[35].

1.3.Prostate specific antigen (PSA)

The wide spread use of PSA screening since the late 1980 coupled with improved diagnostic techniques and increased disease awareness, has led to a diagnosis of prostate cancer at earlier stages and at a younger age than in the pre PSA area [36]. The risk of prostate cancer increases gradually as the PSA value increases from more than 4ng/ml to higher values [37]. The higher proportion of pathologically organ-confined cancers due to early detection increases the likelihood of cure, which may result in an overall decrease of mortality from PCa. Large-scale prospective screening studies are underway to test, whether this promise holds true [7,38]. PSA serum level at the time of diagnosis is also considered a prognostic marker [39,40]. PSA levels are also monitored for early detection of recurrence after therapy (surgery, radiation, or androgen withdrawal) [41].

1.4. Therapy of prostate cancer:

1.4.1. Localized prostate cancer

Localized prostate cancer can be treated with a curative intent (TMN stage T1&2). Radical prostatectomy is suggested to patients with clinically organ confined disease, a life expectancy of 10 or more years but no surgical contraindication [42]. Radiation therapy provides an alternative to radical prostatectomy. The major side effects of these therapies include urinary incontinence and impotence. The incidence of these side effects has decreased in the past years due to technical improvements and new medical therapies. Watchful waiting can be an appropriate choice in selected patients in order to avoid overtreatment in slowly growing or clinically silent prostate cancers [7]. In this approach, patients with early stages of PCa remain untreated but are carefully monitored for progression of disease. This strategy should be considered in case of focal prostate cancer with not more than one single focus of non high-grade cancer in the prostate biopsies, and in patients in whom the natural life expectancy is lower than the expected benefit that may be achieved by aggressive therapy. Such patients may not benefit from aggressive therapy but experience a reduction of quality of life due to the side effects.

1.4.2. Locally advanced PCa

Locally advanced PCa refers to a tumour that is no longer confined to the prostate gland but has not yet metastasised to regional lymph nodes nor to more distant sites. The treatment options are palliative surgery, radiotherapy and androgen suppressing therapy. Radical prostatecomy is usually not performed in patients with clincial evidence of non organ confined disease, since cure can only rarely be achieved in these patients.

1.4.3. Metastatic prostate cancer

Unfortunately, despite early diagnosis, still many PCa progress to metastatic disease. Androgen ablation is the standard therapy of these cancers Since androgens are the main growth and survival factors in prostate cancer withdrawal of androgens reduces the tumour size due to cellular death and decreased proliferation in androgen dependent prostate tumours [43]. Androgen withdrawal can be achieved by classical orchiectomy or pharmaceutically. Pharmaceutical suppression of testosterone production may be accomplished with the use of estrogens, antiandrogen, and agonists and antogonists of luteinizing hormone-releasing hormone (LHRH). Today, orchiectomy and LHRH agonists are most commonly used. LHRH agonists effectively reduce testosterone to castration levels by repression of the hypothalamic – pituitary – gonadal axis. Initially, almost all prostate cancer patients respond well to androgen withdrawal with a reduction of tumor size and alleviation of symptoms [44].

1.4.4. Androgen independent ("hormone refractory") prostate cancer (AIPC)

Initial clinical response to androgen withdrawal is almost inevitably followed by progression towards androgen independent growth after a few months or years with progressive clinical deterioration and ultimately death [44]. These androgen independent prostate cancers (AIPC) are characterized by the lack of sensitivity to any type of hormonal manipulation in the presence of androgen deprivation [45]. For decades, no therapeutic option was available to prolong survival in these advanced cancers. Recently, two large phase 3 trials have demonstrated an overall survival advantage for patients treated with docetaxel-based regimens as compared to the best standard of care [46,47], and other novel therapeutic approaches are under investigation [48].

1.4.5. Molecular mechanisms of androgen independence

Androgen independence may be either complete independence of androgens as growth factors, or it may be tolerance of the low androgen levels present after androgen withdrawal therapy. Although the tumour is independent of androgens at high physiological concentrations, the tumour cells may still dependent on activity of the androgen receptor. There are several mechanisms of aberrant activation of androgen receptor. Gene amplification of the androgen receptor (AR) has been found to induce increased gene expression [49]. As a consequence, lower levels of residual androgens, which are still present after androgen withdrawal therapy, may trigger activation of the androgen receptor [50]. A second mechanism is mutations of the androgen receptor. These mutations may either increase affinity to androgens, or reduce specificity of the androgen receptor allowing estrogens, other steroids or even antiandrogens to bind and activate the androgen receptor [51-53]. A third possibility is ligand independent activation of the receptor by intracellular signalling pathways. One prominent pathway which is involved in androgen independent activation of the androgen receptor is the ErbB2 induced activation of RAS/ ERK1/2 MApK pathways and PI3K/ AKT pathways [54-57]. PTEN represses activity of the androgen receptor and cell proliferation [58]. Thus loss of PTEN function may therefore facilitate tumour growth. Indeed, PTEN mutations and gene deletion are common in specimens from patients with advanced and hormonally treated prostate cancer [59].

Also IL-6 dependent activation of MAPK and Stat3 pathways may lead to ligand independent activation of the AR [60]. Interestingly increased IL-6 serum levels have been reported in prostate tumour patients [60]. Similar results have been obtained with other growth factors such as the keratinocyte growth factor and the insulin-like growth factor-1 [61].

In addition, complete bypass of androgen receptor pathway is possible, though this seems to be less common [62,63]. For example, there is evidence that overexpression of the apoptosis

inhibior Bcl-2 and neuroendocrine differentiation might provide growth advantage to prostate cancer cells under hormone withdrawal [64].

1.4.6. Molecular genetics of prostate cancer

Since cancer is often based on genetic alterations, the detection of chromosomal changes can pinpoint critical genes and highlight mechanisms of cancer development and progression. Comparative genomic hybridization (CGH) is a technique, which allows screening the whole genome for DNA sequence copy number alterations [65]. Previous CGH studies have revealed several frequent chromosomal alterations in prostate cancer including loss of 8p, 13q and 16q, and gain of 8q [66-70]. CGH is especially instrumental for pinpointing chromosomal loci that can undergo DNA amplifications [71]. CGH has lead to the identification of more than 30 previously unknown amplification sites in various tumor types [71]. High-level amplifications can highlight genomic sites containing activated oncogenes with potential prognostic and therapeutic importance. This has been exemplified by the amplification of the HER2 gene in breast cancer. The HER2 status has become a routinely used predictor for therapy response to antibody-based therapy against the HER2 receptor [72].

In prostate cancer, the discovery of androgen receptor (AR) gene amplification provides an example how a genome-wide survey, followed by a focused study at one chromosomal site led to the identification of a novel mechanism of prostate cancer progression, and to a marker for improved prediction of therapy response. After the identification of an amplification site at Xq11.2-q12 in 20-25% of hormone-refractory prostate cancers the AR was identified as the most likely target of this amplicon by fluorescence in situ hybridization using gene-specific DNA probes [50,66]. AR amplification has only been found in prostate cancer and is almost exclusively restricted to hormone-refractory disease [50]. AR amplification is likely to enable the tumors to maximize the effect of the remaining low levels of adrenal-derived testosterone

after orchiectomy by increasing the number of AR density in the tumor cells [73]. Accordingly, AR amplified hormone-refractory prostate cancers have been shown to better respond to second-line total androgen blockage than tumors without AR amplification [74]. Other high-level gene amplifications have been reported in advanced prostate cancers [66,70,75]. They include the prostate stem cell antigen (PSCA), RAD21 and KIAA0196 at 8q24 [76,77], the p40 subunit of eukaryotic translation initiation factor 3 (eIF3) at 8q23 [78], and Cyclin D1 [79] and INT2/FGF3 at 11q13 [80]. The chromosomal region 3q25-q27 was also frequently gained in prostate cancer by CGH, and subsequent comparative PCR analysis showed amplification of several genes in this region including SOX1, IL12A, SLCA2, and MDS1 [81].

1.4.7. 10q22 Amplification

Amplification at 10q22 has been reported in prostate cancer[82], osteosarcoma[83], bladder cancer[84], non-small cell lung carcinoma[85], and breast cancer[86]. Especially in prostate cancer the 10q22 amplification was only found in late stages of the disease[82]. Interestingly, there is a frequent deletion observed at 10q (most likely q23-25) [82,87]. This region comprises the prominent tumour suppressor PTEN, suggesting that deletion of 10q is most likely driven by deletion of this gene[87]. Originally the amplification at 10q22 was discovered in a comparative genomic hybridisation (CGH) screening approach in prostate cancer[82]. The amplification was subsequently mapped using yeast artificial chromosomes (YAC) as FISH probes (pers. Comm. L. Bubendorf) in the cell line PC-3. The mapped region spanned more than 16 Mb. It showed an amplification followed telomerically by a reduction of copy number (deletion).

1.5. Goal of the study

The goal of the study was to identify a gene that drives the amplification at 10q22 in clinical prostate cancer. To achieve this, we planned to screen the region for a peak of amplification in

order to pinpoint putative amplification target genes. The greatly increased gene dosage in case of amplification typically leads to increased gene expression, which could uncouple high gene expression from cellular regulation [88]. In a second approach, genes mapped to 10q22 by the genome sequencing project were assayed in a real time PCR for comparison of gene dosage and expression. We compared gene expression of the model cell line PC-3, which contains an amplification at 10q22, with not amplified control cell lines (BPH-1, LNCaP, CWR22R). By taking the results of these two approaches we expected to narrow the selection of candidate genes. Considering known biochemical and cell biologic properties of these candidates, a hierarchy would be established to assay the genes on cellular levels for oncogenic properties. Ideally, experimental modulation of the activity if the candidate gene protein would response in altered growth rate of the model cell lines.

1.6. Potential amplification target genes at 10q22

1.6.1. KCNMA1 (Large-conductance Ca^{2+}-activated potassium channel)

We describe this gene in more detail than the other genes at 10q22 since it was subsequently selected as the major target of our project.

KCNMA1 encodes for the pore-forming α-subunit of the BK channel, also referred to as Maxi K^+ channel. BK channel is assembled from 4 large α-subunits that build the K+ pore. This assembly is a fully functional BK channel that allows K+ currents of 100-300pS inducing hyperpolarisation of the cell [89] It contains a voltage sensor in the transmembrane domain, which induces opening of the channel in response to depolarisation of the membrane. Additionally, it includes a intracellular calcium sensitive domain (c-terminus) [90]. The gene KCNMA1 covers 0.7 Mb at the genomic locus 10q22 [91]. It contains 27 exons. The current full length cDNA published spans >11kb of sequence [92]. Only the first 3730 bases are considered to contain the coding sequence. The full length α-subunit has a molecular weight of 130 kD.

One to four regulatory ß-subunits may associate to this complex of 4 α-subunits [93]. These proteins are encoded by four individual genes named KCNMB1-4 [94-98]. These subunits affect the membrane potential that causes opening of the channel and provide interaction domains for binding of ligands. For example, iberiotoxin (ibtx) is a peptid toxin that specifically interacts with the BK channel in a competitive manner [99]. The regulatory ß 1 subunit allows interaction with and blocking by ibtx, whereas expression of the ß 4 subunit provides resistance against ibtx [100,101]. 17 ß -estradiol has been shown to interact with the extracellular domain of the BK channel, most likely through the ß 1 subunit [102]. Binding of 17 ß -estradiol and structurally related molecules such as tamoxifen, induce activation of the channel [102].

Activity of the BK channel may be influenced by alternative splicing [91]. For example, inclusion of the stress regulated exon (STREX) causes the protein kinase A (PKA) to inhibit activity of the BK channel, whereas removal of the STREX exon causes PKA to activate the channel [103]. A second site of alternative splicing generates a α-subunit that contains a dominant motif that causes retention of the channel at the endoplasmatic reticulum.[104]. This splice variant may provide insights into molecular mechanisms that cause cytoplasmatic localisation of the BK channel in presence of serum and allows translocation to the cellular membrane in response to serum starvation [105]. Interestingly expression of BK channel has been shown to peak in G1 [106]. Surprisingly, cells arrest in S-phase, rather than in G1 phase, when BK channel activity is inhibited [105]. Consistent with these data, it has been shown that BK channel activity may contribute to the maintenance of DNA synthesis by increasing mitogen-induced increase of intracellular Ca(2+) concentration [107]

Taken together, the BK channel system provides a collection K+ channels with distinct molecular properties from which a cell may select the subpopulation that fits its needs best.

Activity of the BK channel has been found to be crucial in regulation of vascular tone, neuronal excitability, neurotransmitter release, endocrine function, innate immunity, and

hearing [108-112]. In addition, functions in regulation of cell size and cell survival are suggested . Interestingly, a mouse strain containing genomic deletion of KCNMA1 is viable and fertile [113].

1.4.2. Other Genes at 10q22 with a possible role in cancer progression

VDAC2 (voltage dependent anion channel 2): VDAC2 encodes one of the two human isoforms of the voltage dependent anion channel [114]. This may bind to and inactivate Bak [114,115]. Dispalcing BAK from VDAC2 by tBID, BIM or BAD enables oligomerisation of BAK and thereby induces apoptosis [115]. In addition, overexpression of VDAC2 protein has been shown to inhibit apoptosis [115].

PLAU (uPA, urokinase plasminogen activator): PLAU has been linked to carcinogenesis [116]. uPA is a extracellular protease involved in matrix remodeling, which might facilitate metastasis [117]. Binding of the urokinase activator to its receptor, uPAR, may trigger a Ca2+ releasing intracellular signaling cascade [118]. Hypothetically, this activates other Ca2+ regulated proteins at 10q22 including the BK channel Calcineurin, and Calmodulin Dependent Kinase 2 (CamK2). PLAU has previously been suggested as an amplification target at 10q22 in prostate cancer [119]. Both pharmacological inhibition and molecular knock down by siRNA has been shown to reduce matrix invasion of uPA expressing cells[119,120]. Inhibition of uPA activity with specific inhibitors has been shown to reduce growth of prostate cancer xenografts[121]

RAI17 (Retinoic acid-induced gene 17): This gene was not considered in the initial planning of our study, as it was mapped to 10q22 only in the year 2003 [122]. RAI17 interacts with the AR as shown by cotransfection and immunoprecipitation in simian kidney cell lysates[122]. A strong intrinsic transactivation domain was identified in the C-terminal proline-rich region of

RAI17. In human prostate cancer cells, RAI17 augments the transcriptional activity of AR. Moreover, RAI17 colocalizes with AR and SMALL UBIQUITIN-LIKE MODIFIER 1 (SUMO1) at replication foci throughout S phase and is capable of enhancing attachment of SUMO to the AR in vivo. Studies using sumoylation-deficient AR mutants suggested that the augmentation of AR activity by RAI17 is dependent on the sumoylation of the receptor. These data suggest that RAI17 is a coregulator of AR[122]. Several other androgen coactivators such as TIF2 or SCR1 or AIB1 have been suggested to play an active role in androgen independent growth of PCa. It is assumed that overexpression of these factors might enhance AR response to low levels of androgen or broaden specificity of the AR similar to AR mutations. This might allow activation of transcription and cellular growth by AR in the setting of castration [49]. Thus RAI17 qualifies as another very interesting amplification target at 10q22.

CAMK2G (Calmodulin Dependent Kinase 2 gamma): CAMK2G encodes a catalytic subunit of the Calmodulin Dependent Kinase (CamK2) [123]. CamK2 has diverse roles in virtually all cell types and it is regulated by a plethora of mechanisms. Some of these functions may provide growth regulatory stimuli to the cell. For example, CamK2 directly interacts to and phosphorylates Raf1, which provides a link between Ras/Raf/Erk and CamK2 pathways[124]. This pathway leads survival and proliferation of the immortalised thyroid cell line TAD-2 in response to interaction to fibronectin [125,126]. Recently, CAMK2G has been shown to be involved in regulation of the assembly of the mitotic spindle [127].

PPP3CB (Protein phosphatase 3, catalytic subunti, calcineurin B): PPP3CB encodes the ß-isoform of the catalytic α-subunit of the protein phosphatase 3 [128]. Calcineurin, i.e. protein phosphatase 3 is assembled from the catlytic α-subunit, a regulatory ß-subunit and calmodulin[129]. The main function of calcineurin is dephosphorylation of the transcription

factor nuclear factor of activated T-cells (NFAT), which allows translocation of NFAT to the nucleus and transcriptional activity. NFAT regulates activation of T-cells. So far, calcineurin was mostly studied in immunology as it is the target for the immunosuppressive therapy with cyclosporin A. Calcineurin B is also involved in development and function of the nervous system, cardivascular function, signalling in sceletal muscle, and angiogenesis [129]. Inhibition of calcineurin has also been shown to prevent VEGF induced migration and angiogenesis. Calcineurins might also play a role in cancer, although the detailed mechanisms remain to be elucidated. α and β isoforms of calcineurin A (catalytic subunit) have been found to be expressed at a significantly higher level in colon cancer as compared to benign tissue [130]. Calcineurin has also been found to increase expression of Matrix-Metalloproteinase 2 (MMP2) [131]. Calcineurins have a much higher affinity for Ca2+ than CamK2. Thus, it is assumed that calcineurins respond to long term low-level increases of Ca2+, while CamK2 is assumed to respond to short term high level increases of Ca2+ concentration (spikes) [132,133].

MYST4 (Morf): MYST4 encodes a histone acetyl transferase [134] and has been implicated in development of leukaemia by structural and functional interaction with Runx2 [135].

ANX7 (Annexin A7, Synnexin): AnxA7 encodes a membrane associated protein that is involved in membrane fusion and may also act a voltage dependent Ca2+ channel [136,137] Transfection of the wild type gene into human prostate cancer cell lines (LNCaP and Du145) leads to reduced tumour growth and reduced matrix invasion [138]. In addition, expression is reduced in metastatic and locally recurrent Pca. In addition, tumour-suppressor properties of Anx7 have been demonstrated in Anx7 (+/-) mice [139]. Thus, Anx7 is unlikely to be an amplification target at 10q22. These data from prostate cancer contrast with data from breast cancer, where overexpression of Anx7 has been suggested to be involved in metastasis [140].

PSAP: Prosaposin (PSAP) is a precursor of 4 saposins and has growth- and invasion-promoting activities [141,142]. Besides PLAU, PSAP is another gene that has recently been found to be amplified in PC-3 and some advanced prostate cancers [143]. Prosaposin has been reported to activate p42/44 and SAPK/JNK signaling pathways of MAPK and to upregulate expression of PLAU/PLAUR in prostate cancer and stromal cells [142]. This makes PSAP an interesting putative amplification target gene. PSAP was not taken into further consideration in our project because it is located at 73.2-73.3 MB on chromosome 10q22.1, which was not within our selected region of interest.

1.4.3. Other Genes at 10q22 with no apparent role in cancer

SFTPA1& SFTPA2 (surfactant, pulmonary-associated protein A1&2):Pulmonary surfactant is a phospholipid-protein complex that serves to lower the surface tension at the air-liquid interface in the alveoli of the lung [144,145] It is essential to normal respiration [146,147]. Inadequate amounts of surfactant at birth, a frequent situation in premature infants, results in respiratory failure[148].

Polr3a (polymerase RNA III polypeptide A): This gene encodes the largest subunit of the human RNA polymerase 3 [149]. So far, there is no evidence for a cancer related function of Polr3a.

RPS24 (ribosomal protein S24): This gene encodes the 40S ribosomal subunit protein S24 [150]. It is organized into 6 exons and is differentially spliced to yield 2 isoforms, S24a and S24c, that are present at varying ratios in different tissues [151].

DUSP13 (dual specificity phosphatase 13): This gene has only recently been identified and allocated to 10q22. It encodes two dual-specificity protein phosphatases (DSPs) that are involved in postnatal development of specific tissues including including testis and skeletal

muscle[152,153]. Interestingly, the DUSP13 locus is the first gene from which two distinct proteins of the same family are expressed using alternative open reading frames[153].

ADK (Adenosine kinase): ADK catalyzes the transfer of the gamma-phosphate from ATP to adenosine, thereby serving as a potentially important regulator of concentrations of both extracellular adenosine and intracellular adenine nucleotides [154]. No cancer related properties have been reported.

SEC24c: In yeast, the Sec23-Sec24 complex is a component of coat protein II (COPII)-coated vesicles that mediate protein transport from the endoplasmic reticulum. SEC24C is one of several mammalian proteins that show structural and functional homology to yeast Sec24 [155,156].

NDST2 (N-Deacetylase/ N-sulfotransferase 2): N-deacetyl/ N-sulfotransferase 2 catalyses the initial step in the processing of heparin polymerase to heparin sulphate or heparin [157]. Targeted disruption of the mouse Ndst2 gene by homologous recombination suggest an essential function in mast cells [158,159].

VCL (Vinculin): Vinculin encodes a cytoskeletal protein that crosslinks integrins and E Cadherins to F-actin [160,161] suggesting a function in cell adhesion. Vinculin has been demonstrated to inhibit cellular motility and apoptosis [162]. The exact mechanism of how vinculin regulates apoptosis is unclear. However, it has been shown that vinculin allows stabilisation of PTEN protein [163]. In addition vinculin null (vin-/-) cells show upregulated activity of extracellular signal-regulated kinase (ERK) [162]. These data may explain observations of tumour suppressor properties of vinculin in SV-40-transformed Balb/c 3T3 cells [164].

MOYZ (Myozenin): Myozenin is a protein that localizes to the z-line of skeletal muscle [165]. Expression was found to be highest in skeletal muscle. Until today no other function for myozenin have been reported.

There is also a number of genes at 10q22 from which no functional data are available, including ZNF503 (zinc finger protein 503), COMTD1 (catechol-O-methyltransferase domain containing 1), DUPD1 (dual specificity phosphatase and pro isomerase domain containing 1), SAMD8 (sterile alpha motif domain containing 8), AP3M1 (adaptor-related protein complex 3, mu 1 subunit), FUT11, KIAA0913, and CHCHD1 (coiled-coil-helix-coiled-coil-helix domain-containing protein 1).

Taken together, different genes with oncogenic properties in prostate reside at 10q22. This suggests that several genes, rather than just one single gene, might drive amplification at 10q22. This model fits with theories of operon like organisation of the human genome [166]. It has previously been shown that genes that are expressed under the same conditions are frequently colocalised to one genomic region [167]. However a few cases of clusters of functionally related genes are known, for example the globin gene cluster or the hox gene cluster. This colocalisation in a distinct region of the genome would facilitate regulation of gene expression by means of chromatin organisation [167]. In a simplistic view, activation of one given cellular pathway would only require activation of a limited number of genomic regions rather than the whole genome. In this context, it is highly interesting that three of the proteins encoded in the amplified region at 10q22 are regulated by Ca2+: Calcineurin, CamK2 and the BK channel. Also PLAU might be a part of this group because it may trigger a signalling cascade leading to intracellular increase of Ca2+ [118].

2. Results

2.1. Amplicon mapping: BAC FISH on 10q22 TMA reveals no distinct peak of amplification

In a previous analysis, the region of interest at 10q22 had been defined by mapping a YAC contig onto the human genome sequence published on www.ensemble.org. This contig was used to analyse the amplicon of PC-3 providing a first scaffold of the 10q22 amplification profile in PC-3. The two BACs RP11-464F9 and RP11-137H2 were selected as borders of the region of interest. Currently, these BACs are mapped to 75.1Mb and 82.2 Mb, respectively. The mapping process lead to the selection of a BAC contig, which contains 70 individual BACs **(Fig. 1A)**. It covers 7 Mb of genomic sequence. Sequence data of the BAC were obtained and aligned in order to verify the contig. The sequencing software was not able to align the BAC into one contig. Overlapping of the small contigs retrieved from alignment was manually verified confirming that the selection covers one large contig. The BACs were obtained from the Sanger Centre (Cambridge, UK). We chose BACs as FISH probes rather than much larger YACs. BACs allow much higher resolution of the amplification profile, which may lead to a much more specific selection of amplification target genes.

When this study was initiated, 9 genes were mapped to the region of interest. They included Annexin 7 (ANX7), Calcineurin 3B (PPP3CB), the calcium/calmodulin-dependent protein kinase (CaM kinase) II gamma (CAMK2G, KCCG_ Human), urokinase activator (PLAU), Vinculin (VCL), Adenosinekinase (ADK), monocytic leukaemia zinc finger protein related (MORF, MYST4), potassium channel, calcium activated, large conductance subfamily M, alpha member 1 (KCNMA1), and discs, large homolog 5 (DLG5) **(Fig 1A)**. Thus, these genes were selected as first candidate genes. The evaluation of the amplification profiles by FISH did not reveal the expected anatomy of the 10q22 amplification. The overlay of all amplification profiles obtained from the 10q22 TMA showed a flat profile with no distinct

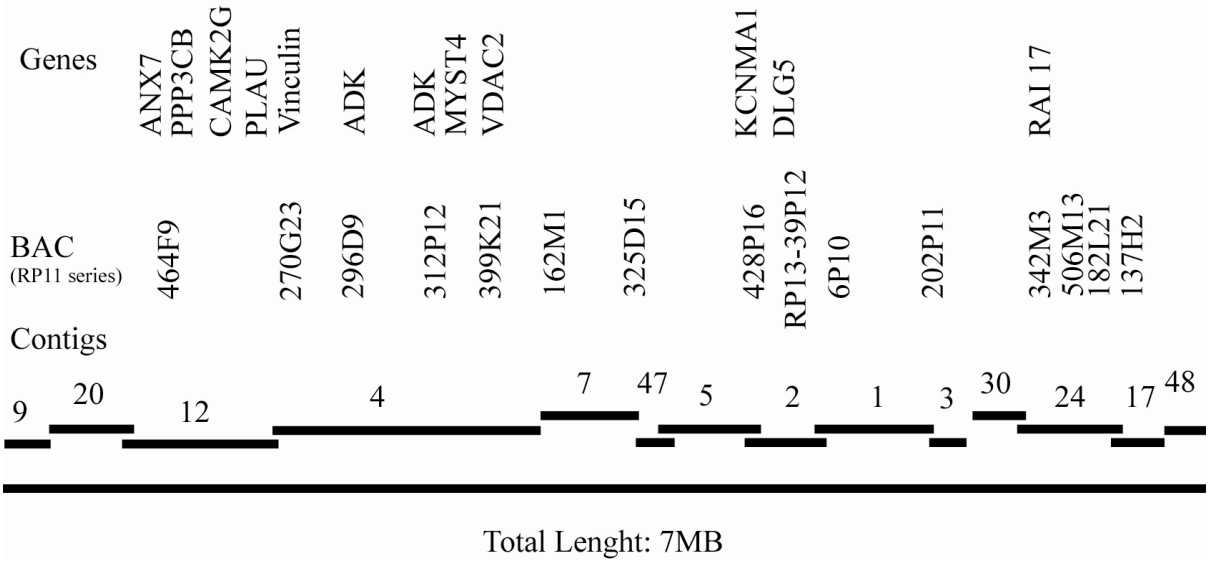

(A)

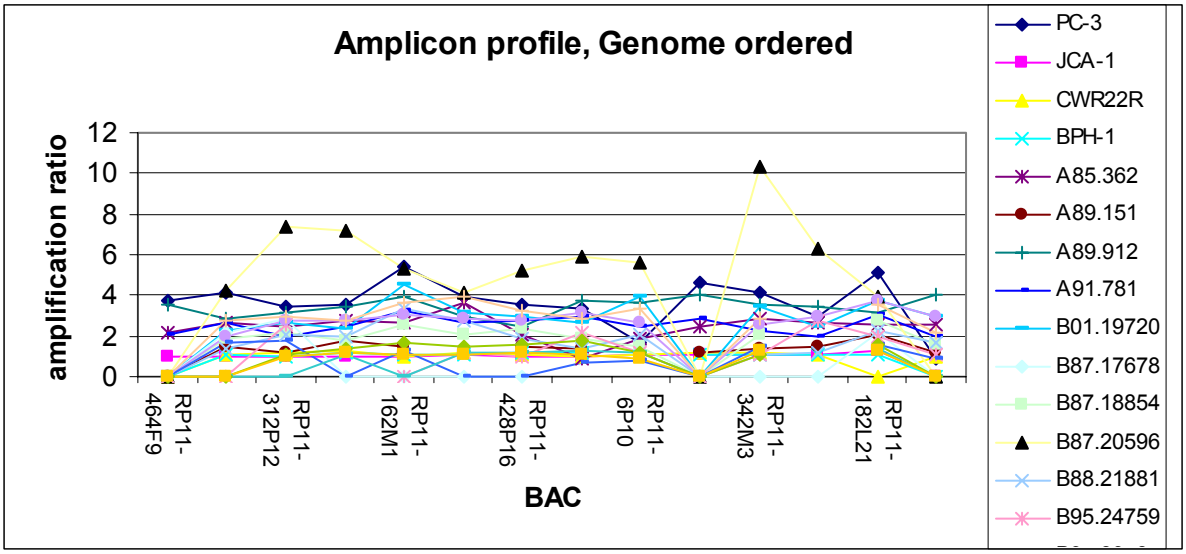

(B)

Figure 1: 10q22 Amplification. (A) The region of interest was defined between the BAC RP11-464f9 and RP11-137H2. The numbered bars indicate contigs assembled by the sequencing software. These contigs overlap to one large contig. Currently the region of interest is mapped between 75.1 Mb and 82.2 Mb on chromosome 10 (source: ensemble.org).
(B) Amplification profile of the 10q22 amplicon. In a series of 12 clinical human PCa biopsies there was no distinct peak of amplification. In addition the cell line PC-3 (amplified at 10q22) and control cell lines BPH-1 JCA-1, CWR22R (all not amplified) were included. Amplification ratio= 0 indicates that this FISH probe could not be evaluated in this case.
Y axis: amplification ratio = average of Bac FISH probe signals/ average of centromer 10 (CEP 10) probe signals

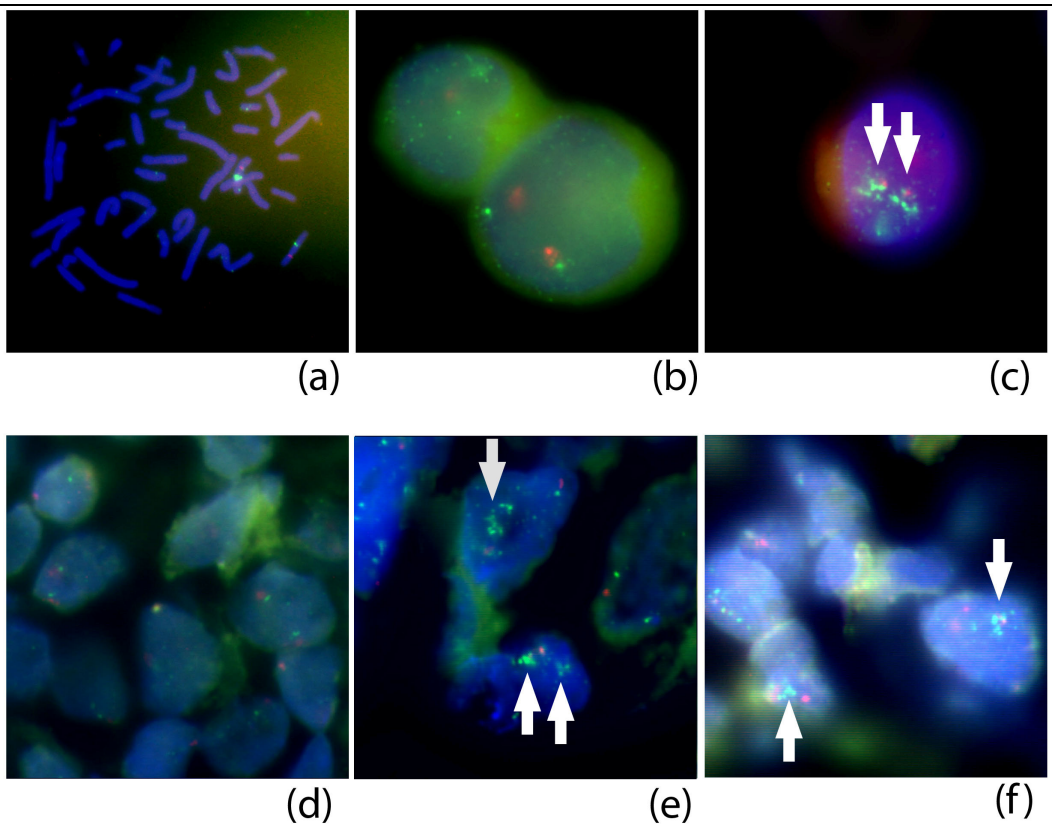

Figure 2: FISH probe RP11-428P16 covering KCNMA1 genomic sequences.
(A) Hybridisation on human reference cell lines shows specificity of the FISH probe. Metaphase chromosomes of a single cell show hybridisation to the 2 chromosomes 10 and no hybridisation to other chromosomes. Chromosome 10 is highlighted by hybridisation of a probe specific for its centromer.
(B) Hybridisation on BPH-1 shows the normal ratio of 2 centromers per cell and 2 probe signals near by.
(C) Hybridisation on PC-3 shows amplification of the FISH probe (arrows). Amplification is seen as a cluster of probe signals next to the centromer 10 signals. PC-3 is polysomic for chromosome 10 (not shown in this image).
(D) Hybridsation on a human PCa with a ration of 2/ 2 (FISH probe/ centromer).
(E+F) Hybridisation on two human PCa with amplification seen as cluster of probe signals (arrows)
The figure shows false colour images. Blue: DNA (DAPI stain), green: FISH probe RP11-428P16, red: centromer 10 probe (CEP10, Vysis)

peak of amplification **(Fig 1B)**. Thus, this experiment did not allow narrowing down the selection of candidate genes. However, there was a region with a tendency towards higher amplification ratios next to the BAC RP11-162M1 and RP11-325D15. A second region of higher amplification was located at the BAC 182L21 However, these differences were small. There are no genes that have been mapped to the BAC RP11-162M1 and RP11-325D15, yet. Also, there is no known gene mapped between these to BAC except a predicted transcript named CJ011_HUMAN. So far, no function has been ascribed to this transcript. The gene KCNMA1 resides 0.4Mb to the telomeric side of RP11-325D15. Similarly, there is no known

gene mapped to the BAC RP11-182L21. Next to this BAC there is the gene SFTPD. The BAC RP11-428P16 was selected for further study because it contains genomic sequences of the gene KCNMA1. In the mean time, two interesting genes VDAC2 and RAI17 have been mapped to 10q22. VDAC2 locates to the BAC RP11-399K21, and RAI17 is close to the BAC RP11-342M3.

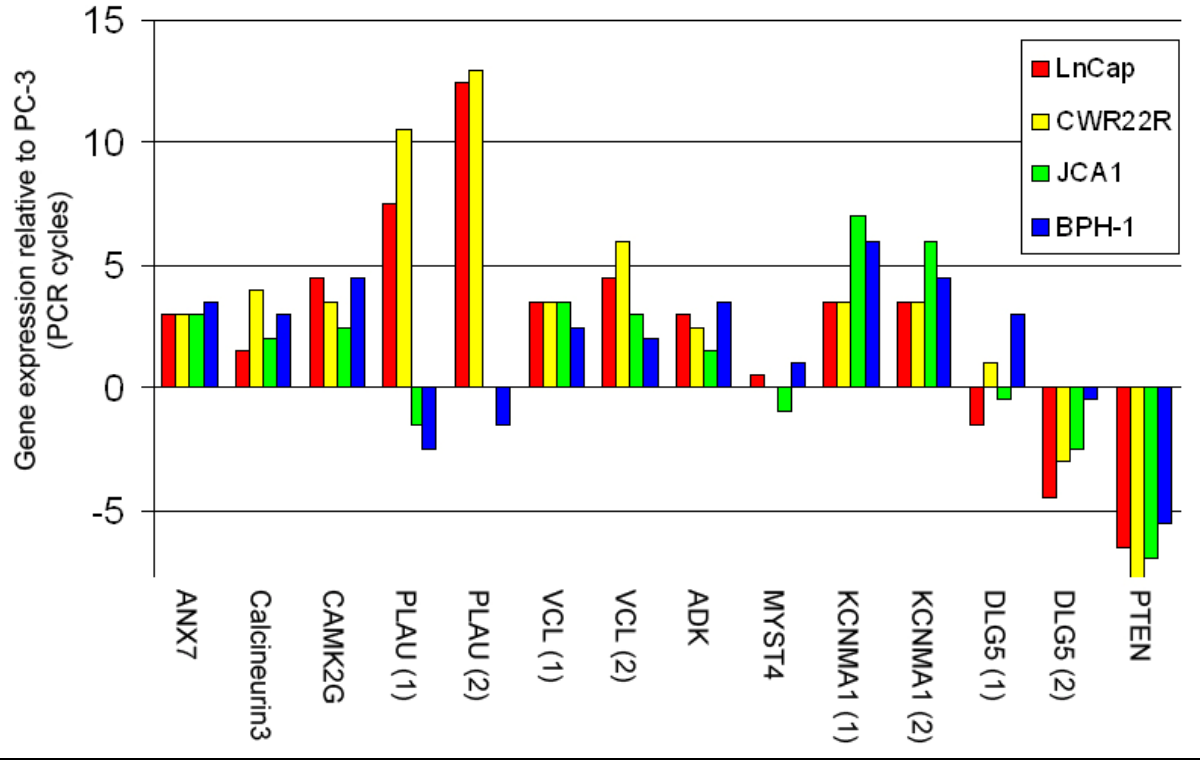

Figure 3: Expression of genes at 10q22 in human PCa cell lines.
Highest relative expression was found for PLAU when PC-3 was compared to LNCaP and CWR22R but not
The figure shows expression of LNCaP, BPH-1, CWR22R, and JCA-1 compared to PC-3. Values > 0 indicate increased expression in PC-3, values < 0 indicate reduced expression in PC-3. y axis: numbers of PCR cylces corrected for expression of GPDH.

2.2. Expression of 10q22 genes in model cell lines

In addition to FISH analysis, we performed a gene expression analysis of the selected candidate genes located at 10q22 using a LightCycler based RT PCR assay. For this experiment we obtained 5 human cancer cell lines including PC-3, LNCaP, BPH-1, CWR22R, and JCA-1. In the mean time JCA-1 has been shown to be a bladder cancer cell

line by means of cytogenetics [168]. Thus, data obtained for JCA-1 were considered of reduced significance for this project.

All cell lines except CWR22 grew readily in Optimem +10% FCS. These surface adhering cells accept non-coated plastic (Falcon cell culture flasks) as substrate. In contrast to PC-3, LNCaP, and BPH-1, CWR22 required higher cell density for rapid growth.

Analysis of mRNA expression by LightCycler RT-PCR revealed that all of the selected genes were expressed at a higher level in PC-3 as compared to the control cell lines, with the exception DLG5 and MORF (BAC RP11-312P12) **(Fig 3).**

Among all tested genes, PLAU was most strongly expressed in PC-3 as compared to LNCaP and CWR22R. However, there was no increased expression of PLAU in PC-3 relative to BPH-1 and JCA-1. In case of a amplification target gene, one would ideally expect a more consistent association between gene amplification and overexpression.

KCNMA1 showed the second highest expression in PC-3, although the difference to other genes was small. Importanly, all of the 4 control cell lines expresses KCNMA1 at a lower level than PC-3. Expression of PTEN was assayed as a reference, as it is known to be deleted at 10q24 in PC-3. As expected, expression was markedly lower in PC-3 as compared to the control cell lines **(Fig 3)**.

Although mRNA expression analysis did not clearly highlight a putative amplification target, the consistent association between amplification and overexpression of KCNMA1 made it the most interesting candidate for further analyses. The experiment allowed excluding DLG5 and MORF as putative amplification target genes.

category	Number of cases	KCNMA1 amplification (n)	KCNMA1 amplification (%)
Benign prostatic hyperplasia	33	0	0
High-grade PIN	32	0	0
T1a/b	43	0	0
T2	62	0	0
T3/4	10	2	20.0
Lymph node metastases	17	0	0
Distant metastases	47	7	13.0
Hormone-refractory local recurrences	45	10	22,2

Table 1: Prevalence of KCNMA1 amplification in prostate cancer. FISH analysis of 298 specimens on a prostate specific tissue microarray (TMA). The BAC RP11-428P16 was used as KCNMA1 specific probe and the centromeric probe for chromosome 10 as a reference. Amplification was defined as a ratio between gene and reference of ≥ 2. BPH = benign prostatic hyperplasia, PIN = prostatic intraepithelial hyperplasia, T1a/b = incidentally detected prostate cancer in transurethral resection for presumed BPH, T2 = clinically organ confined prostate cancer treated by radical prostatectomy, T3/4 = clinically non-organ confined, locally advanced prostate cancer treated with palliative transurethral resection, LN metastases = pelvic or paraortal lymph node metastases.

2.3. FISH on a prostate progression array

Next we assayed the prevalence of 10q22 amplification in clinical prostate cancer. For this assay, the BAC RP11-428p16 that includes genomic sequences of the gene KCNMA1 was selected as a FISH probe. We screened a prostate progression TMA that had been built from 587 individual cases of PCa and 25 controls. In total 262 (45%) samples could be evaluated. A case was considered not evaluable if there was either no probe signal, or no CEP 10 signal, or if there was too high background fluorescence precluded clear distinction of specific from non specific signals.

These data confirmed the previous observation that amplification at 10q22 prevails only in late stages of prostate cancer **(Table 1)**. Amplification was found in T 3/4 stage cancer (2 of 10 cases), distant metastases (7 of 47), and hormone refractory cancer (12 of 45). Surprisingly there were no amplified cases within the 17 regional lymph node metastases (0 of 17). As expected, there were no amplifications in benign prostatic hyperplasia (33 cases), high grade PIN (32 cases), and the early stage prostate cancers at stage T1 (43 cases) and T2 (62 cases).

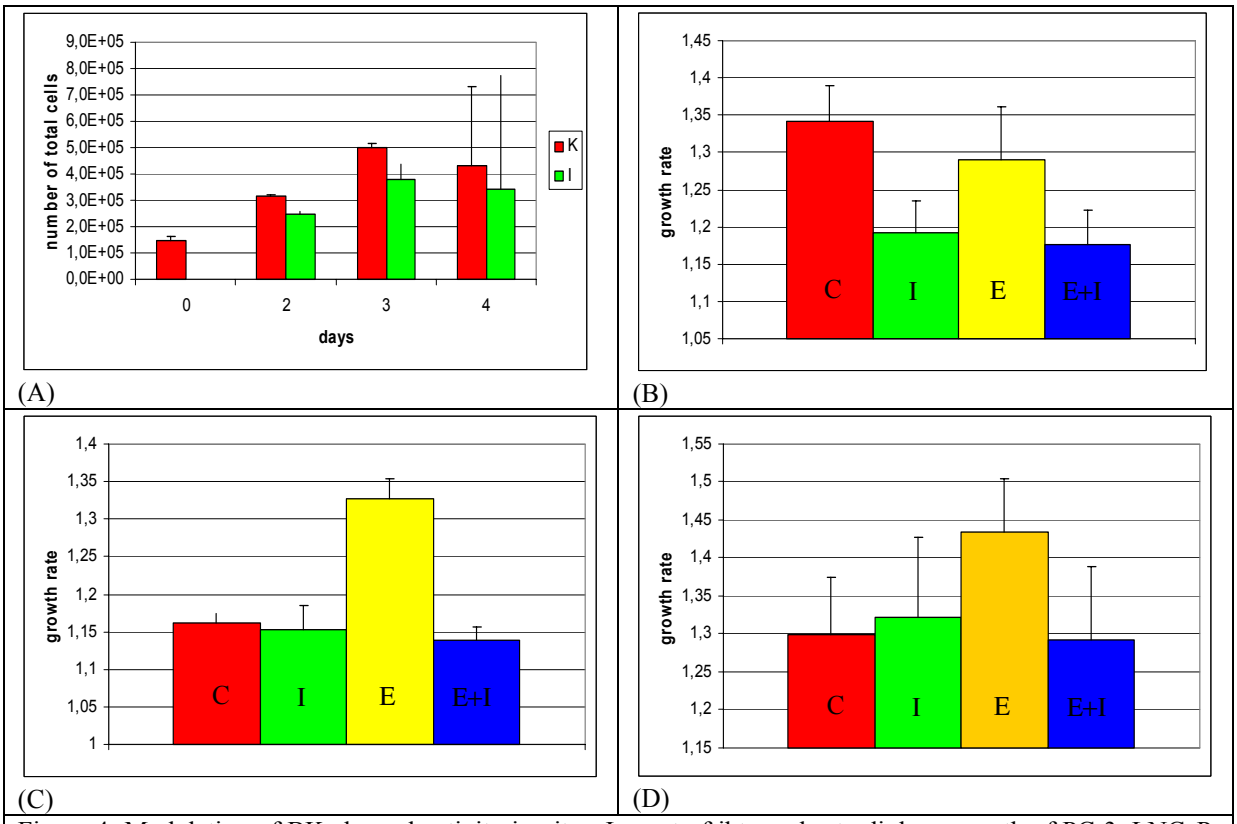

Figure 4: Modulation of BK channel activity in vitro. Impact of ibtx and estradiol on growth of PC-3, LNCaP, and BPH-1.
(A) Growth of PC-3. PC-3 proliferates up to day 3. At day 4 the culture collapses as indicated by the high standard deviation at this time point. Ibtx reduces PC-3 cell numbers significantly but does not prevent proliferation. Y-axis: total number of cells per well.
(B) Growth of PC-3 in response to ibtx and estradiol. Growth of PC-3 is significantly reduced by ibtx. Addition of estradiol does not changed growth of PC-3 significatly and does not override action of ibtx.
(C) Growth of BPH-1 in response to ibtx and Estradiol. Growth of BPH-1 is not change in response to ibtx. Addition of Estradiol increased growth of BPH-1. Combination of estradiol and ibtx does not alter the growth rate as compared to the control.
(D) LNCaP responds in a similar way as BPH-1, though not statistically significant.
C: Control, I: Ibtx, E: 17b-estradiol, E+I: Combination of Estradiol and Ibtx.
(B-D) y-axis: virtual growth rate k from the hypothetical growth curve $A(t)= A0*e^{kt}$. A(t): number of cells at time t, A(0): number of cells at time 0, t: time in days.

2.4. Modulation of BK channel activity affects growth of PC-3 and BPH-1

In this assay we took advantage of the known fact that 17β-estradiol and Iberiotoxin (ibtx) modulate the activity of the BK channel. 17β-estradiol activates the BK channel by interaction with the β1 subunit. In contrast ibtx is considered a highly specific BK channel inhibitor.

For this experiment a specialised medium formulation of Optimem + 10% Albumax was used. Although PC-3, LNCaP and BPH-1 grow well in Optimem + 0.4% Albumax (see **Fig. 4a** in case of PC-3) none of these cell lines adhere readily to the uncoated surface of Falcon 6 well

plates when seeded in this medium. As a consequence the cells were seeded in standard growth medium (Optimem +10% FCS). After one day, the medium was changed to Optimem +1%FCS. The next day, the medium was changed to Optimem+ 0.4% Albumax containing the drugs if needed. Thus, this protocol includes a step of serum starvation that may influence the results. However, since all samples in the experiment were equally treated we considered the influence of this protocol on the results to be of minor importance.

The obtained data were used to calculate a virtual growth rate k from a hypothetical experimental growth curve $A=A^0*e^{kt}$. A and A_0 were numbers of cells, t is time in days. There was a significant reduction of the growth rate of PC-3 in response to treatment with ibtx **(Fig. 4B)**. Although this experiment confirmed involvement of the BK channel in regulation of rapid growth of PC-3, the observed reduction of cell growth was relatively small. Ibtx treated PC-3 continue to proliferate at high division rate. In contrast to PC-3, growth of BPH-1 was not altered in response to ibtx **(Fig. 4C)**. Taken together, the data suggest that PC-3 (in contrast to BPH-1) expresses a pool BK channel that is constitutively active at the conditions of growth in this experiment.

Addition of 17β-estradiol to BPH-1 significantly stimulated growth of this cell line **(Fig 4C)**. Importantly, the stimulation of growth induced by 17β-estradiol could be prevented by administration of ibtx. This finding suggests that 17β-estradiol induces growth in BPH-1 through activation of BK channel **(Fig 4C)**. In contrast growth of PC-3 was not stimulated by 17β-estradiol **(Fig. 4B)**. However, when estradiol and ibtx were added together the effect of ibtx was retained. Thus, in contrast to PC-3, BPH-1 may contains a pool of BK channels that are inactive at the growth conditions of this experiment but may be recruited to stimulate growth of this cell line.

The response of LNCaP was similar to the response of BPH-1. However, the high variation of the raw data prevented the analysis of statistical significance of growth in LNCaP **(Fig. 4D)**.

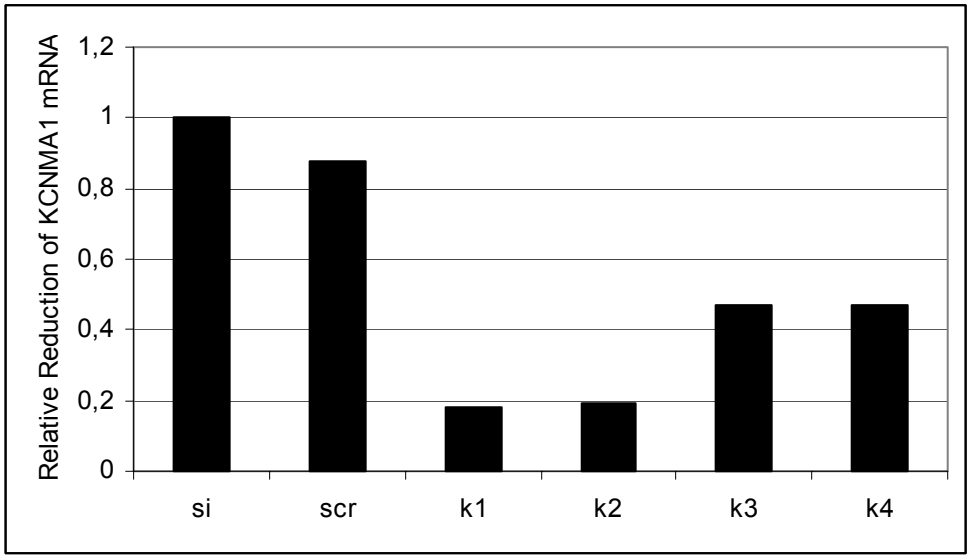

(A)

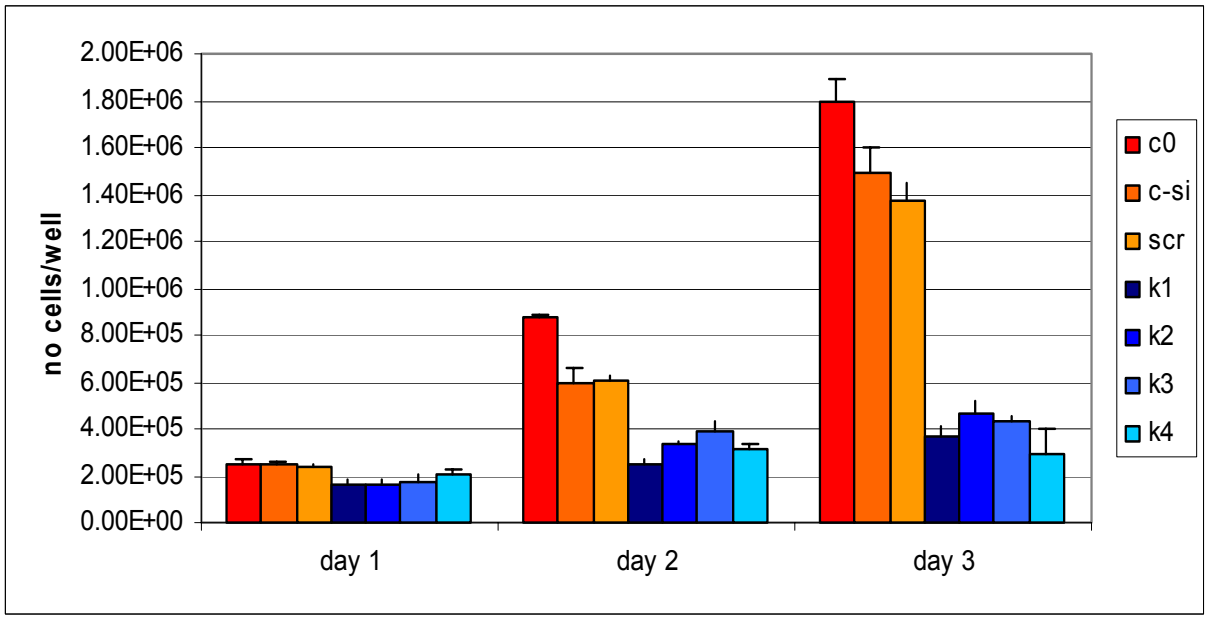

(B)

Figure 5: Anti KCNMA1 siRNA in PC-3.
(A) Reduction of KCNMA1 mRNA in response to anti KCNMA1 siRNA K1-4. Transfection of siRNA K1 and K2 reduced KCNMA1 mRNA levels to <20% when compared to non-transfected cells (c-si) or cells transfected with scrambled sequence RNAi (scr). Transfection of siRNA K3 and K4 reduced KCNMA1 mRNA levels to <50%. Figure is drawn to be relative to the expression in the control (c-si). Thus all 4 siRNA K1-4 significantly reduce KCNMA1 mRNA in PC-3.
(B) KCNMA1- RNAi using all 4 active siRNA K1-4 has a pronounced inhibitory effect on PC-3 cell growth. Y-axis shows total number of cells per well.
C0: non treated PC-3, c-si: non-transfected cells, only transfection agent, scr: transfected with scrambled sequence RNAi, K1-4: transfection of siRNA K1-4.

2.5. siRNA

SiRNA technique was applied to study the effect of specific knockdown of KCNMA1 mRNA. The 4 individual siRNAs that were used target different regions of the mRNA. Interestingly, siRNA K2 targets a region that has been implicated in alternative splicing [169,170]. SiRNA lead to a knockdown of KCNMA1 mRNA levels of 2-4 PCR cycles, which corresponded to a reduction of mRNA by 50-80%. Knockdown of KCNMA1 mRNA was achieved by all 4 siRNA molecules tested **(Fig. 5A).** Thus, all 4 siRNA could be used to study contribution of KCNMA1 to cellular growth of PC-3.

Transfection of siRNA slightly reduced growth of PC-3 as compared to the negative control experiments. Both treating the cells with lipofectamine and - even more pronounced - transfection of inactive scrambled siRNA lead to a significant reduction of PC-3 cell numbers at day 3 after transfection (at day 3 c0 vs c-si: p=0,0238, c0 vs scr: p=0,0038, c-si vs scr: p=0,01743; **Fig 5B)**, though PC-3 continued to grow rapidly. PC-3 cells that were treated with any of the active siRNA K1-4 grew very much slower than any of the controls (the p-value is equal or smaller than 0.001 for all combinations of controls versus the active siRNA at day 3; **FIG 5B**). Thus the toxic effect of the transfection is minor when compared to the effect of active siRNA. Notably, some proliferation was retained in siRNA treated PC-3 after siRNA transfection, though at a very low level **(Fig 5B)**. Taken together, these data strongly suggest that the BK channel promotes rapid growth of PC-3, but it is most likely not essential to vitality.

Interestingly, transfection with anti KCNMA1 siRNA had a reproducible effect on the phenotype of PC-3 after four days **(Fig 6)**. The phenotype of untreated PC-3 was a spindle-like, triangular to rectangular cell shape when grown in Optimem + 10% FCS **(Fig 6 A-C)**. It readily adhered to the surface of the culture flask with little cells floating in the medium. Little or no cell to cell interaction seemed to be required for growth of PC-3 because most of the cells grew in an isolated manner with no contact to each other. Similarly, there was no

tendency to grow as nodules or other forms of cellular aggregates at low cellular density. Filopodia were frequently seen at the endings of the spindle. The siRNAs 1, 2, and 4 induced a similar phenotype. After siRNA treatment, the PC-3 cells spread towards a roughly rectangular shape **(Fig 6D, E, and G)**. However, subtle differences of the phenotype were visible for these three siRNAs, making each phenotype unique. Astoningishly, siRNA K3 treated cells looked completely different. These cells became longer and thinner as compared to wild type PC-3 cells **(Fig 6F)**. This finding suggests that the action of the individual siRNAs may differ. Although non-specific action cannot be excluded, these siRNAs might be useful to understand more deeply the diverse function and regulation of the BK channel. However, this was beyond the scope of this study.

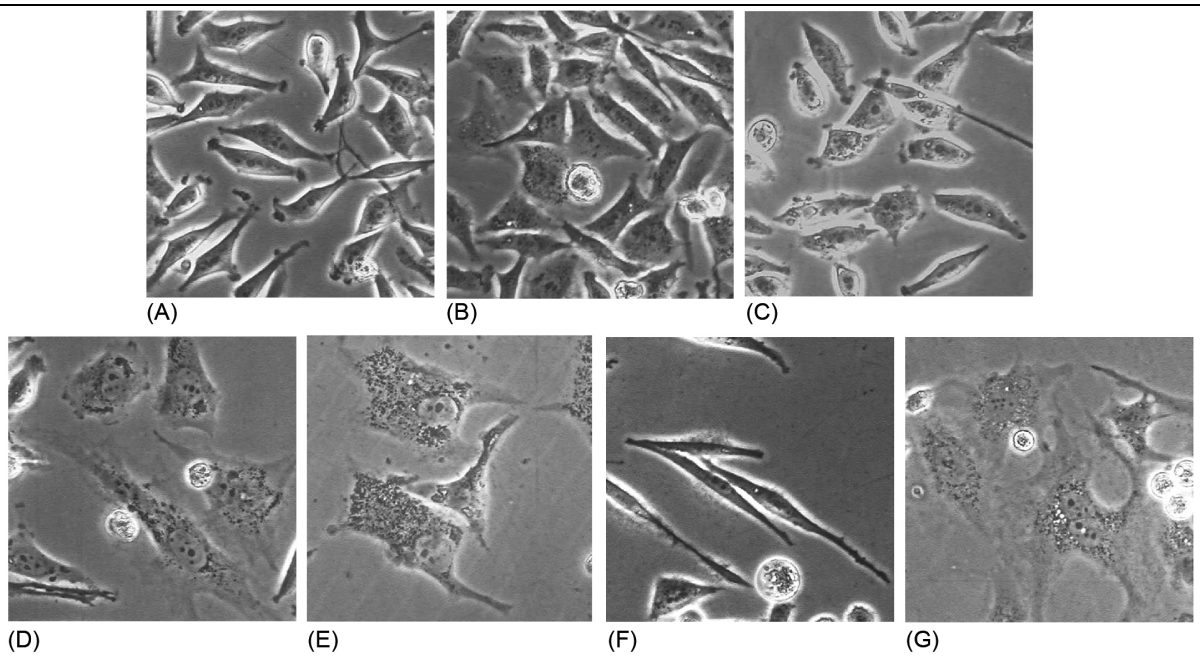

Figure 6: Phenotype of PC-3 4 days after transfection of siRNA.
(A) normal Phenotype of PC-3. The cells were not transfected with siRNA (c0). The cells show a typical spindle like phenotype.
(B) The phenotype of PC-3 treated with transfection agent (c-si) closely resembles the phenotype of (A).
(C) The phenotype of PC-3 transfected with scrambled sequence siRNA (scr) closely resembles the phenotype of (A).
(D) Transfection of siRNA K1: PC-3 cells cover a much larger surface area and show a roughly rectangular cell shape.
(E) Transfection of siRNA K2: PC-3 cells cover a much larger surface area and show a roughly rectangular cell shape.
(F) Transfection of siRNA K3: PC-3 cells form a elongated spindle with reduced diameter and increased length as compared to (A-C)
(G) Transfection of siRNA K4: PC-3 cells cover a much larger surface area and show a roughly rectangular cell shape.

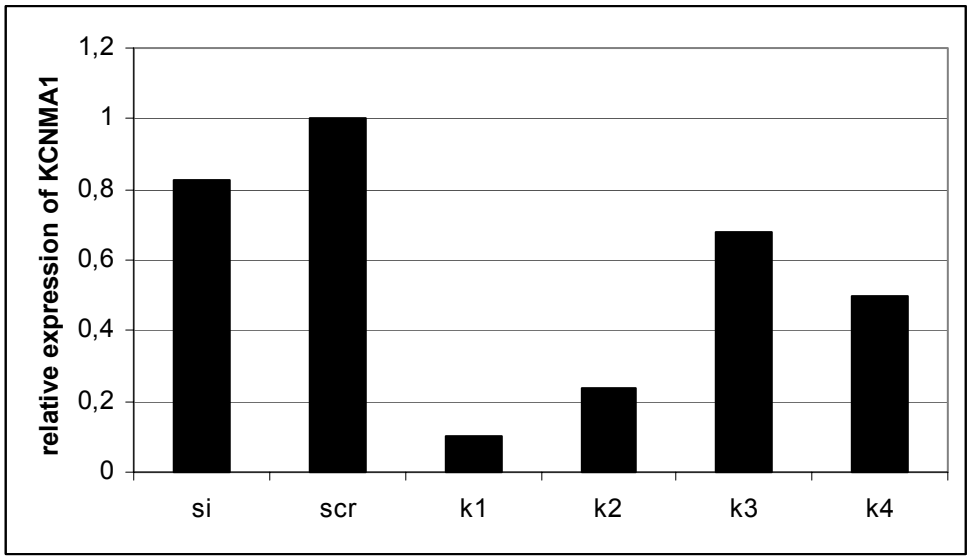

(A)

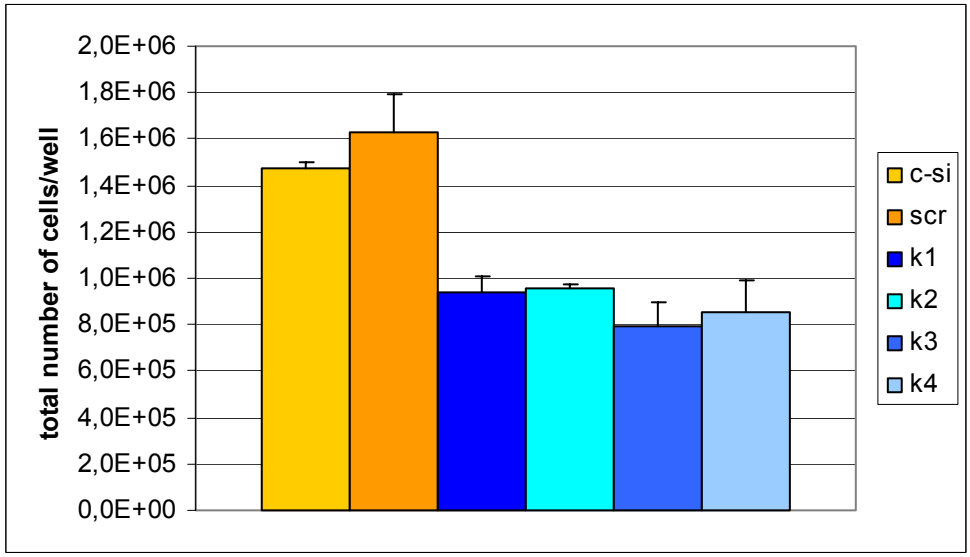

(B)

Figure 7: Anti KCNMA1 siRNA in BPH-1.
(A) Relative reduction of KCNMA1 mRNA in response to anti KCNMA1 siRNA K1-4. Transfection of siRNA K1, K2, and K4 reduce KCNMA1 mRNA to 10%, 23%, or 50%, respectively, as compared to scrambled sequence RNAi (scr). The siRNA K3 reduces KCNMA1 mRNA to only 68% as compared to scrambled sequence siRNA. The y-axis shows relative expression of KCNMA1 as compared to transfection of scrambled sequence siRNA (scr). These data are corrected for expression of G6PD.
(B) KCNMA1- RNAi using all 4 active siRNA K1-4 has an inhibitory effect on BPH-1 cell growth. Y-axis shows total number of cells per well.
c-si: non-transfected cells, only transfection agent, scr: transfected with scrambled sequence RNAi, K1-4: transfection of siRNA K1-4.

LNCaP and BPH-1 were also treated with siRNA. As in PC-3, knockdown of KCNMA1 was verified by quantification of KCNMA1 mRNA. In BPH-1, the siRNAs K1 and K2 lead to a knockdown of mRNA of 4 and 2.5 PCR cycles, which corresponds to a relative reduction of 10% and 23%, respectively **(Fig 7A)**. siRNA K4 induced a reduction of only 1 PCR cycle,

and siRNA K3 had almost no effect with a reduction of only 0.3 PCR cycles, which is still in the range of experimental errors. This minor effect of K3 on BPH-1 was reproduced in repeated experiments.

In BPH-1 there was a growth reduction of about 50% at day 4 after transfection all siRNA **(Fig. 7B)**. Although the effect was much less pronounced than in PC-3, these data suggest that KCNMA1 is also involved in the growth of BPH-1.

In the LNCaP cell line, stable PCR used for RT PCR could not be achieved, precluding reliable mRNA expression analysis after siRNA. We did not obtain specific PCR product using the standard PCR conditions. The reasons for this failure of PCR in LNCaP are not clear. Increasing the elongation time of the PCR from 15 sec to 2 min resulted in PCR products that are longer than the original fragments. As the same PCR protocols worked well for BPH-1 and PC-3 that were run in parallel, the inability to obtain appropriate PCR products in LNCaP might be related to the RNA properties of this specific cell line. Also, changing PCR conditions such as annealing or Mg^{2+} concentration could not solve this problem. Thus, LNCaP could not be used to test the effect of anti KCNMA1 siRNA on growth of cell lines in vitro because we could not verify whether or not siRNA reduces of KCNMA1 expression (data not shown).

2.6. Western blotting

Testing for specificity of the 3 commercially available anti-BK channel antibodies for specificity revealed bands of variable sizes for all antibodies irrespective of the type of lysis buffer. Among the 3 antibodies, APC-107 from Alomone Labs showed brightest signal and lowest background. These tests revealed a mobility shift assay, giving a unique banding pattern for each cell line **(Fig. 8A)**. In PC-3 and BPH-1 a weak band of the size of the full length BK channel α-subunit is visible

Next, we assayed the knockdown of the BK channel α subunit in response to anti KCNMA1 siRNA treatment in PC-3.

The immunoreaction did not reveal any difference in band intensity for all assayed time points and all siRNAs tested as compared to the related controls **(Fig 8B)**. Thus this experiment did not demonstrate reduced BK channel protein in response to siRNA.

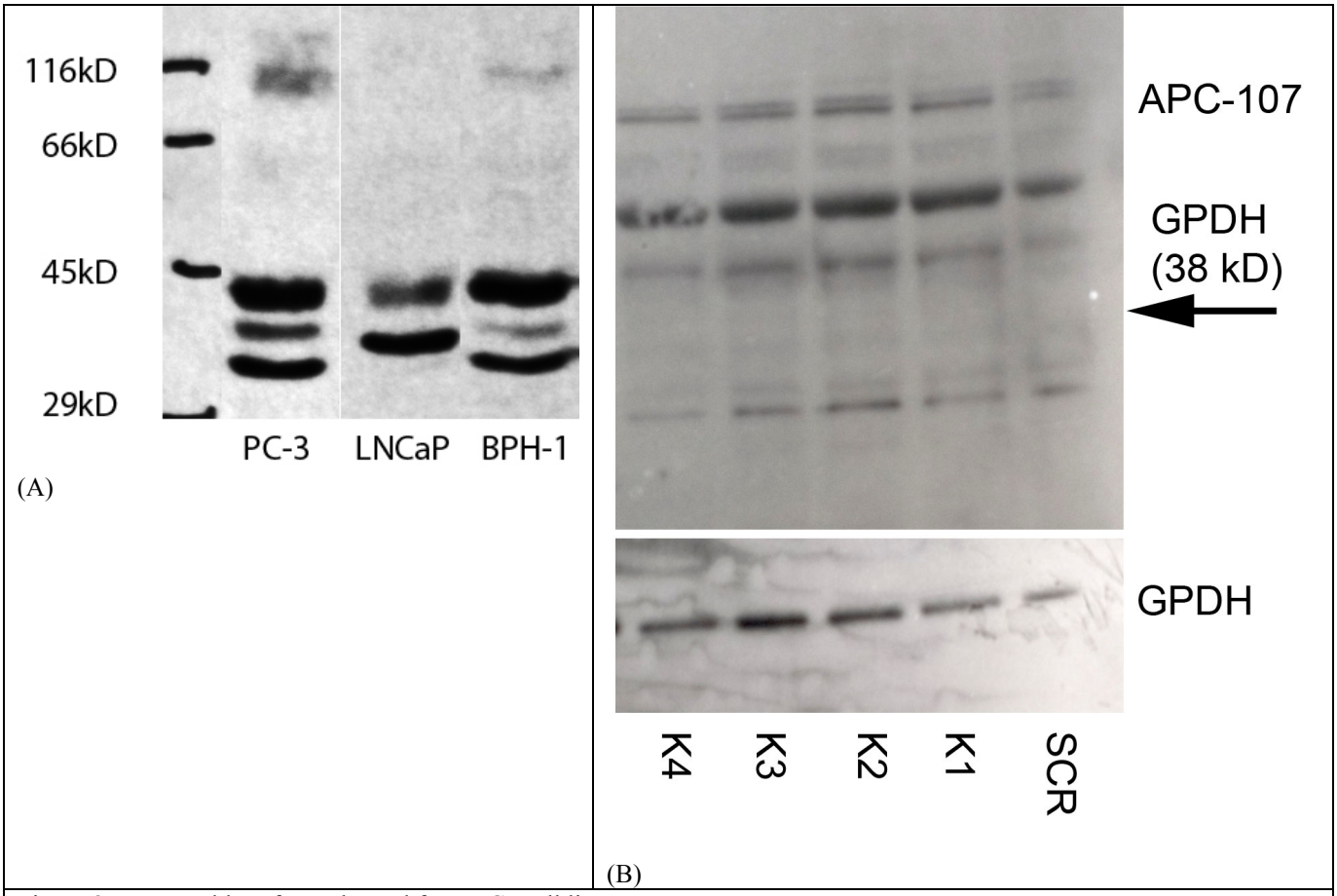

Figure 8: Western blot of BK channel from PCa cell lines.
(A) BK channel of PC-3, LNCaP, and BPH-1 resolved on a 6% acrylamide gel. Each cell produces a distinct banding pattern when BK channel a subunit is resolved using the antibody APC-107 (Alomone labs). The bands show a weak band of full length of BK channel a subunit (indicated by arrow). Bands of lower molecular weight may represent degradation products of the BK channel
(B) siRNA in PC-3. There is no difference in BK channel expression observed in response to siRNA, although knock down of KCNMA1 mRNA was measured (Fig 5a).
The antibody was APC-107. The gel was a precast 4-12% acrylamid gel (Invitrogen).
scr: transfected with scrambled sequence RNAi, K1-4: transfection of siRNA K1-4.

2.7. KCNMA1 expression in human tumours using RT PCR:

During the last few years fresh biopsy material from locally advanced prostate cancer was collected and stored at -70°C at the Institute for Pathology of the University Hospital Basel for molecular analysis including gene expression analysis. The estimated time frame from

surgical tissue removal to freezing ranged from 20 to 40 minutes. It is likely that some variable degree of RNA degradation occurs within this time span. For practical reasons, however, it is almost impossible to cut this time frame much shorter in a diagnostic setting of a pathology laboratory. From our series of fresh frozen specimens, we were able to identify 2 individual human prostate cancers with KCNMA1 gene amplification by FISH to the frozen TMA. We compared mRNA expression of KCNMA1 from PC-3, 2 tumours with gene amplification, 7 tumours without gene amplification, and two cases of BPH. The tissue for RNA extraction was punched from blocks of frozen tissue. The tissue area was selected to contain maximal amount of the desired tissue avoiding surrounding stroma if possible. The 2 tumors with KCNMA1 amplification did not have an increased expression of KCNMA1 as compared to the not amplified tumours (**Fig 9**). In contrast, the samples of BPH had increased expression of KCNMA1 up to the level of PC-3. Thus, we found no correlation between gene amplification and mRNA expression of KCNMA1 in human tumours.

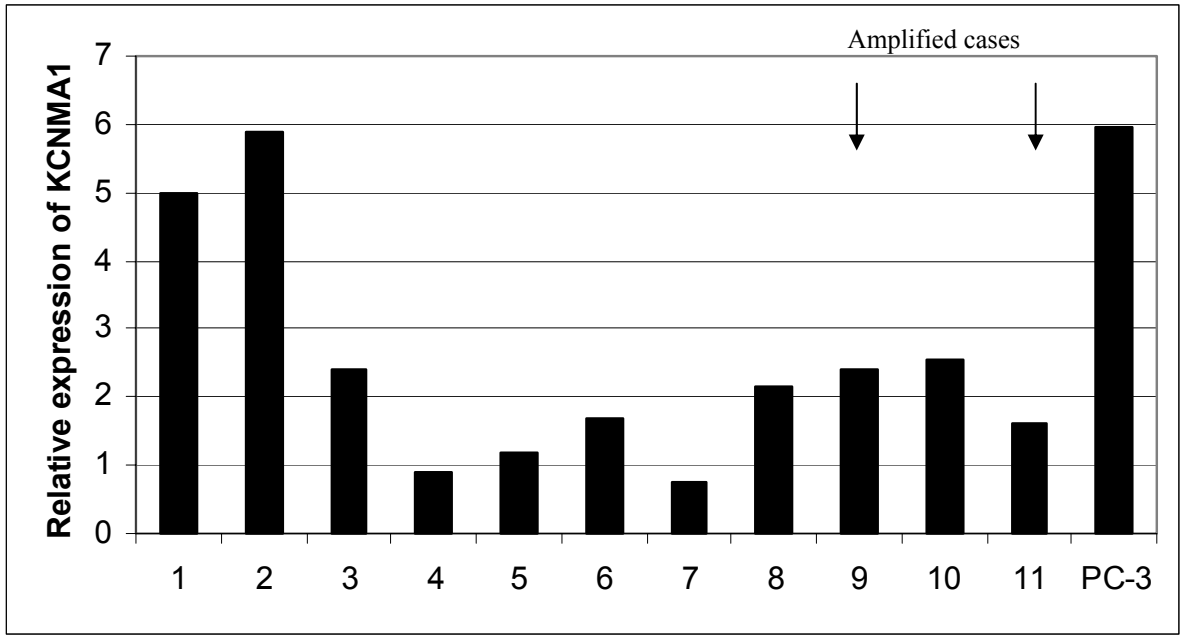

Figure 9: Expression of KCNMA1 gene products in human PCa and PC-3.
The figure shows expression of KCNMA1 gene products in PC-3, 2 cases of BPH (1& 2), and 9 cases of human PCa (3-11). Amplified cases are cases 9 and 11. BPH has much higher expression of KCNMA1. Amplified cases do not show increased expression as compared to not amplified cases of PCa.
Y-axis: Expression of KCNMA1 corrected for expression of the reference gene G6PD, in PCR- cycles. Increased values indicate increased relative expression of KCNMA1

3. Discussion

3.1. Screening the Amplicon at 10q22

Gene amplification is considered a critical mechanism of carcinogenesis in different tumour types [171]. Prominent examples are amplification of ERBB2 in breast cancer and amplification of the androgen receptor (AR) in prostate cancer [50,172,173]. In these cases amplification of the proto-oncogenes uncouples expression from cellular regulation, which leads to increased expression and uncontrolled activity of the proteins. In the case of ERBB2, increased expression leads to constitutive activation of the receptor tyrosine kinase and ERBB2 dependent signalling[174,175] Similarly, increased expression of AR allows activation of AR at the very low cellular concentration of androgens that remains after androgen withdrawal [50]. Amplification allows activation of downstream pathways independently of proper external stimuli [49,176]. Amplifications can pinpoint to genes with oncogenic properties. Thus, the study of amplified regions on structural and functional levels may lead to the discovery of novel oncogenes.

It has repeatedly been shown that one amplicon can contain more than one amplification target gene that may contribute to selection. For example, co-amplification of GST-pi, INT2 and HSTF1 has been described at 11q13 in breast cancer [177], and coamplification of GRB7 and ERBB2 in Barrett's carcinoma [178].

3.2 Structure of the Amplification at 10q22

In general, the structure of an amplicon, i.e. its profile, which is the ratio of amplification plotted on the scaffold of the human genome, is assumed highly predictive in the context of selection of amplification target [179-181]. Accordingly, a first attempt was to screen the region at 10q22 for a peak of amplification. The method of choice was fluorescence in situ hybridisation (FISH) because it allows a good compromise between relatively small probes (bacterial artificial chromosomes have an average length of 100-200 kb) and high throughput

when used on tissue microarray (TMA) [182]. We used a specialised TMA that was enriched for prostate cancer with 10q22 amplification to define the amplification profile at 10q22 and narrow down its peak.

Due to the flat profile of the amplification with no distinct peak, we were not able to further narrow down the initial selection of candidate genes (**Fig 1B**). This amplification shows relatively low amplification ratio and covers a large region of the genome of greater than 7 Mb. Based on the existing amplification profiles as shown by comparative genomic hybridization in PC-3 and in previously analyzed clinical prostate cancers, we would have rather expected the presence of an amplification peak. The reasons for the absence of a distinct peak in our FISH analysis remain unclear. It could be that the Vinculin BAC probe that had been used to select amplified tumours for this specialized TMA was not optimal. Vinculin was not highly amplified and may reside close to the base of the amplicon. The amplification at 10q22 is large when compared to many other known amplifications. The factors that determine the size of an amplicon are not well defined but include physical factors such as the specific location of fragile sites. Fragile sites are known to favour amplification and determine the form and the boundaries of amplicons [183]. Accordingly, recurrent chromosomal breakpoint at 10q22 has previously been observed to participate in deletion and translocation in several prostate cell lines including PC-3 [184]. Interestingly, the gene MYST4 at 10q22 has been found to be involved in a translocation in a subgroup of acute myeloid leukaemia [185].

In addition, one could speculate that the size of the amplicon increases as the number of selecting amplification target genes increases. Thus, a large amplicon such as the one at 10q22 may contain several genes that jointly act as a selective force. This view is supported by previous CGH array data where two types of amplicons have been identified including large amplicons spanning up to several Mb of genomic sequence and small amplicons with only one or two genes [186].

Taken together, there are at least two forces that determine amplification: a region in the genome that is prone to genomic rearrangement, and positive selective forces that favour inheritance of the amplification such as oncogenes. Since these two forces cooperate to generate an amplicon, the selective force may not need to be located on the peak region, as long as it is included in the amplicon.

3.3 Clinical Prevalence of Amplification at 10q22 in Prostate Cancer

It has previously been shown that most amplifications in prostate cancer occur at late stages of progression but only rarely in localized cancers [187,188]. For example, MYC amplification has preferentially been found in metastases, and androgen receptor is almost always restricted to advanced, androgen insensitive prostate cancer [50,75,187]. Similarly, we found amplification of the BAC RP11-428p16 only in advanced stages of prostate cancer (**Table 1**). Chromosomal instability may be a prerequisite of amplification as it also develops during prostate cancer progression. The fact that amplification is absent or rare in earlier stages due to mechanistic reasons does not exclude a role of amplification target genes in carcinogenesis at this stage. Such genes may exert an effect on tumour growth and early progression in early stage tumours through lower level of expression due to low-level increase of gene dosage or through epigenetic mechanisms.

3.4 KCNMA1 as putative amplification target gene.

In this project we selected KCNMA1 for further studies based on the following pieces of evidence: 1. There is a consistent association between KCNMA1 amplification an mRNA overexpression in PC-3 and control cell lines in vitro (**Fig2B,C, Fig 3**). 2. KCNMA1 amplification is present in a fraction of advanced prostate cancers *in vivo*, and 3. The known specific blocker ibtx and the activator 17β-estradiol were available for functional studies [100,102]. The fact that ibtx significantly inhibited growth of PC-3 strongly suggests that the BK

channel contributes to growth of PC-3 and that the channel is active at standard growth conditions (**Fig 4**). This finding is consistent with the results from previous studies on other cell lines and different K+ channels, where an involvement of K+ channels in carcinogenesis has been suggested [189-193]. Importantly, the growth inhibitory effect of ibtx was restricted the PC-3 but absent in BPH-1 and LNCaP, which is in favour of a functional importance of amplification driven overexpression of KCNMA1. However, the growth stimulatory effect of 17β-estradiol on BPH-1 and LNCaP could be blocked by ibtx suggest that BK channel may also be essential to the growth stimulation in these cell lines without KCNMA1 amplification. We assume that the growth stimulatory effect of 17β-estradiol in these cell lines is to a great part mediated through activation of the BK channel rather than by activation of steroid receptors [194]. In addition our result suggests that both BPH-1 and LNCaP contain a pool of BK channels, which - in contrast to PC-3 -is inactive at standard growth conditions (**Fig 4**).

3.5 Anti KCNMA1 siRNA suggests a role of KCNMA1 in rapid growth of PC-3 and BPH-1

In order to further strengthen the data we performed anti KCNMA1 siRNA to knock down expression of KCNMA1 mRNA (**Fig 5, Fig 7**). This experiment lead to reduced growth of both PC-3 and BPH-1, suggesting that both cell lines require KCNMA1 expression for rapid growth. The positive effect of KCNMA1 mRNA knockdown in the non-amplified cell line BPH-1 may question the importance of KCNMA1 as amplification target. However, BPH-1 has considerably lower KCNMA1 expression that may induce rapid growth if it is properly stimulated. Furthermore it contains a functionally different pool of BK channels than PC-3. It appears that a minimum level of KCNMA1 expression is required for rapid growth of these two cell lines, independent of amplification.

It has recently been reported that K+ channels of intermediate K+ gating potential (IK channel) rather than BK channels are active in PC-3 [195]. This report, however, can not be compared to our data, because the authors performed the measurements in Ringer solution

whereas we used normal growth medium in our experiments. It is known that the type of fluid environment can greatly influence the properties of the cells [196,197]. For example, it has been shown that the presence of serum growth factors in the medium significantly alters the membrane potential of the cells [198]. This altered membrane potential modulates activity of voltage dependent K+ channels, such as the BK channel [199].

In addition to functional changes we observed an interesting morphologic effect of siRNA in PC-3 but not in BPH-1 (**Fig 6**). All four siRNA molecules targeted against KCNMA1 mRNA resulted in a unique and reproducible phenotype in PC-3. This suggests that the phenotype is dependent on the siRNA molecule used. These individual phenotypes may be caused by a knock down of individual subsets of KCNMA1 mRNA that could be generated by alternative splicing. Thus, these phenotypes may reflect inactivation of different subsets of BK channels. However this remains hypothetic and needs to be studied in more detail. For example, it needs to be tested whether these phenotypes are not just side effects of the individual siRNA molecule without being related to specific knock down of KCNMA1.

It is noteworthy that K2 targets a region of the BK channel that is obviously involved in alternative splicing (splice site 1) [169,170]. If this siRNA targets only a subpopulation of the whole KCNMA1 mRNA, it might not only reduce BK channel expression but also alter its activation and deactivation kinetics.

It is known that transfection of long double stranded RNA molecules can have unspecific effects. These effects can include a general block of gene transcription and induction of apoptosis in mammals [200,201]. Such unspecific effects are unlikely in our study as the length of our siRNAs did not exceed 21 bp [202]. Crosshybridization to RNA from other genes might be another cause of non specific effects of siRNA. Such crosshybridization was most unlikely in our study as blasting of the siRNA target sequences against the human genome did not

produce a specific hit besides the human KCNMA1 mRNA. Unspecific knockdown of genes due to undefined mechanisms of siRNA action is more difficult to control and not yet predictable for individual siRNAs . We used scrambled sequence siRNA as a well established control for this purpose. However, the use of specific controls may be more appropriate, i.e. siRNA with point mutations as compared to the active siRNA K1-4. Such specific controls are sometimes recommended to increase the reliability of the experiments. In contrast to random sequence controls they might better control unspecific action of the siRNA.

Based on our current data it is not yet possible to decide whether or not KCNMA1 is an oncogene. However, the presence of gene amplification in advanced prostate cancer in vivo, the association between amplification and mRNA over-expression in cell lines, and growth effect of blocking KCNMA1 activity *in vitro* strongly suggest that KCNMA1 plays a role in the progression of prostate cancer. Nevertheless, we do not claim that KCNMA1 is a major player in a complex network of regulation of cellular growth, survival and other cancer related function. We rather believe that KCNMA1 contributes to growth by supporting general growth regulating functions of the cell.

3.6 No correlation between amplification and overexpression in human prostate cancer

Despite the line of experimental evidence that suggests KCNMA1 as a candidate amplification target at 10q22 in prostate cancer; there are data that question this hypothesis. Surprisingly, there was no correlation between expression and amplification in a limited series of human tumours (**Fig 9**). If true, these data would reject our hypothesis of amplification driven increase of expression of KCNMA1 in human tumours and suggest that the found association may be a clinically irrelevant property of prostate cell lines. However, the data are problematic in several ways. First, the number of cases (2 amplified cases, 10 controls) is too low to allow definitive conclusions. Quality of the RNA is another concern. The tissue specimens did not provide enough RNA for testing RNA quality prior to cDNA synthesis.

Although the material was frozen at -70°C immediately upon arrival at the institute for pathology, the time span from surgical removal of the tissue to the arrival at the laboratory may have been variable, with an estimated range from 20 to 40 minutes. Thus, it cannot be excluded that some of the RNAs were degraded [203]. Taken together, the analysis of KCNMA1 expression in clinical tumours and its association with gene amplification needs to be repeated under optimized condition with a higher number of tumours before we can draw final conclusions.

3.7. BK channel activity is reduced in response to transfection of siRNA K2

A major limitation of this study was the failure to demonstrate the effect of KCNMA1 mRNA knockdown by siRNA on protein expression (**Fig 8B**). Our experimental model assumes that RNA interference of KCNMA1 reduces activity of the BK channel due to reduced expression of the pore forming α-subunit after specific knock down of the KCNMA1 mRNA (**Fig 5**). Our failure to detect a reduction of BK channel α-subunit by Western blotting or immunocytochemistry may have several reasons. It appears that the three commercially available antibodies that we tested were of inferior quality for Western Blotting. Similarly, a specific immunocytochemical staining reaction was not achieved despite extensive testing on cell lines and formalin fixed tissue specimens. Further work is required to fine tune the experimental conditions of Western blotting for BK channel and to obtain or develop better antibodies. For example, others reported that BK channel extracted from glioma is adversely affected by boiling. [170]. Thus, the boiling in presence of reducing agents that we applied before loading the SDS PAGE might have impaired quantification of BK channel protein knockdown. However, changing the preparation of the lysates before loading the gel did not alter the banding pattern nor the banding intensity (data not shown).

One might also argue that the inability to demonstrate a reduction of BK channel α-subunit on a protein level following siRNA is in favour of unspecific action of siRNA with no effect on BK channel. However, our collaborator Karl Kunzelmann (Department of Physiology, University of Regensburg) found strong indirect evidence that KCNMA1 expression is greatly enhanced in the cellular membrane of PC-3 as compared to BPH-1. In an electrophysiological approach, he could show that BK channel dependent K+ currents in PC-3 are significantly reduced in response to the siRNA K2, as compared control siRNA (unpublished data). Importantly, patch clamp experiments revealed that the density of active BK channels is much higher in PC-3 than in BPH-1. Furthermore, transfection of siRNA K2 in PC-3 significantly reduced both sensitivity to the BK channel blocker paxilline and the amount of BK channels in a randomly selected patch of the cell membrane. Taken together, these electrophysiological data strongly suggest that siRNA K2 reduces expression of the BK channel. The data also support the view that the failure to demonstrate protein expression of BK channel by Western Blot was most likely due to technical problems.

3.8 BK channel meets estradiol in prostate cancer

The known regulation of BK channel activity by 17β-estradiol is particularly intriguing [102]. 17β-estradiol and structurally related molecules, such as tamoxifen, interact with the extracellular domain regulatory subunit β1 of the BK channel and may activate the BK channel[102,204,205]. However, recent data suggest that the regulation of the BK channel by tamoxifen is much more complicated. Apparently, activity of BK channels is inhibited by tamoxifen, if the channels are composed of α-subunits only. In contrast β- tamoxifen may increase the activity of the BK channel when β subunits are present [206].

The role of estrogens in regulation and organisation of the benign prostate may have been underestimated in the past [27]. There is increasing evidence suggesting that estrogens cooperate with androgens to induce PCa[194,207]. In detail, prolonged treatment of adult rodents with

estrogens along with androgens leads to epithelial metaplasia, PIN-like lesions and even adenocarcinoma of prostate[27]. One major effect of androgen ablation therapy is increasing estrogen levels relative to androgens. Taking these observations together, it could be speculated that androgen independent growth of prostate cancer might be triggered by estrogens, i.e. that the tumour cell might become stimulated by estrogens under conditions of androgen withdrawal. This is supported by observations that in an artificial model of LNCaP progression towards androgen independency estrogen regulated genes were activated [208].

In our experiments BK channel was shown to be constitutively active in PC-3, whereas BPH-1 contained a pool of BK channels that could be activated by 17β-estradiol (**Fig 4**). Thus, we propose that increased activation of BK channel contributes to growth either by amplification and overexpression (PC-3) or by activation through 17β estradiol (BPH-1). Interestingly, expression of mRNA of estrogen receptors is detectable in PC-3 and BPH-1 [209]. However, in PC-3 the expression is reported to be as low as in breast carcinomas that are considered negative for estrogen receptor by immunohistochemistry [210]. Our data linking BK channel to 17β estradiol in prostate cancer support the notion that BK channel is an attractive putative target for treatment of androgen insensitive PCa.

3.9. Putative mechanisms of K+ channels in cancer

A growth promoting effect of BK channel is not unique to prostate cancer, but has also been demonstrated in astrocytoma [105 193]. Similarly to our results in PC-3, ibtx decreased growth of the glioma cell line D54-MG [105]. As amplification at 10q22 has not been reported in astrocytoma, other mechanisms may be responsible for KCNMA1 overexpression in this tumour type. Diverse types of K+ channels have been found to be overexpressed and activated in a number of tumour cell lines as compared to benign controls. These include Ca2+- activated K+ currents, Shaker-type voltage-gated K+ currents, the ether-a-go-go (EAG)

family of voltage gated K+ currents, inward rectifier K+ currents, ATP sensitive K+ current and swelling-activated K+ current [211]. These previous reports support the notion that K+ gating is important to regulation of cell growth. The precise mechanism by which K+ channels promote tumour cell growth is still unknown.

It has been known for a long time that tumour cells have different electrophysiological properties than normal cells [212]. In particular, tumour cells have a lower resting membrane potential. Consequently, membrane depolarisation has been suggested an important precondition for unlimited tumour cell growth. A first model predicts that the low membrane potential facilitates Ca2+ influx into the cell due to activation of voltage dependent Ca2+ channels at lower membrane potentials [189]. Intriguingly, several growth hormones such as epidermal growth factor (EGF), interleukin 2 (IL-2), and insulin induce sustained oscillations of membrane potential, which may be important to tumour cell proliferation [189].
In addition, it has recently been reported that survival promoting translocation of transcription factor NFAT (nuclear factor of activated T cells) to the nucleus in response to NFkB (nuclear factor kappa-B) may depend on K+ channel activity[213].

Another putative mechanism by which K+ channels regulate cell growth may be related to changes in cell volume. It is known that activity of K+ channel can lead to a regulatory volume decrease (RVD) [189]. Interestingly, decrease of cellular volume favours polymerisation of the actin cytoskeleton [214]. Such polymerisation of actin cytoskeleton can have profound effects on critical proteins. For example, it favours translocation of CyclinD1 to the nucleus and allows sustained activation of integrin dependent signalling (MAP Kinases) [215].
Taken together, BK channel may lead to activation of growth promoting pathways through RVD and consecutive polymerization of the actin cytoskeleton. However, the mechanisms of

how K+ channels affect tumor cell growth remain hypothetic, and further studies are needed to elucidate the downstream effects of K+ channels.

In addition, K+ exit through K+ channels has been reported to favour in apoptosis, where cell shrinking precedes fragmentation of nuclear DNA [216]. Thus, due to complex interaction with other signalling pathways, K+ channels may play a dual role in both cell proliferation and apoptosis.

In another model, activity of K+ channels leads to activation of intra-cellular growth promoting factors. For example, it has previously been observed that epidermal growth factor activates K+ channels in myeloblastic leukaemia, which leads to activation of ERK2 MAP kinase. A mediator that links activity of K+ channels to activation of ERK2 has not been defined, yet [211].

3. 10. Significance of this thesis

The goal of this thesis was to identify a target of 10q22 amplification, and to validate its potential as a diagnostic and therapeutic target in prostate cancer. We propose that the potassium channel KCNMA1 has properties of an amplification target gene based on the following pieces of evidence: First, KCNMA1 is amplified in a fraction of late stage prostate cancer but not at early tumour stages. Second, there amplification is associated with overexpression in prostate cell lines. Third, inhibition of KCNMA1 by a specific blocker or siRNA technique reduces growth of the KCNMA1 amplified cell line PC-3. However, there is a missing piece to be added before a true oncogenic function of KCNMA1 can be considered. Unfortunately, we were not able to demonstrate altered expression of KCNMA1 on a protein level, most likely due to technical problems in the Western Blotting experiments. It will also be necessary to demonstrate such an association in clinical tumours. In addition, the growth inhibition in the PC-3 cell line by ibtx was statistically significant yet comparatively minor. In case of a drugable target, one would ideally demand a more pronounced effect. Optimization

of growth conditions in future experiments may allow demonstrating a greater effect of BK inhibition. The therapeutic potential of BK channel blockers has been recognized by pharmaceutical companies given the role of potassium channels in cardiovascular and neurological disorders, and in cancer. For example, the potassium channel TASK3 (KCNK9) at 8q24.3 has recently been found to be amplified in 10% and overexpressed in 44% of breast cancers [190]. While ibtx is a toxin with no clinical utility, there are other BK channel blockers under development for clinical application (confidential information).

3.11 Future directions

The hypothesis that KCNMA1 is a putative amplification target gene at 10q22 should be strengthened by future experiments. Our study opens the following routes of future research:

1. Knockdown of BK channel protein in response to siRNA should be demonstrated.

2. The link of KCNMA1 amplification and increased expression in clinical specimens requires further study. For this purpose additional clinical specimens should be obtained and analysed. An antibody that allows semi-quantitative analysis of BK channel protein of formalin fixed tissue would be highly desirable. Ideally, it would allow direct correlation of KCNMA1 amplification and BK channel expression using a large scale TMA

3. Amplification of 10q22 should be studied in more detail. FISH is an appropriate technique for this purpose, especially if applied to TMAs. High resolution screening for DNA sequence copy number changes across 10q22 could be achieved by high density BAC arrays or SNP arrays.

4. This study focuses on KCNMA1 as amplification target gene. The role of other interesting genes at 10q22 including VDAC2, PSAP, RAI17 and PLAU should be analysed.

5. The regulatory mechanisms by which ion channels are involved in functional regulation or execution of the cell cycle need to be elucidated. In the case of the BK channel, increased expression in late G1 phase might be related to the regulatory volume decrease that is

observed in G1 phase. However, is has also been shown that inhibition of BK channel in D54-MG cells arrests the cells in S phase [105].

4. **Materials& Methods**

4.1 Bacteria, Generation of Fish probes& Analysis of Gene Amplification

Clinical specimens

The 298 formalin-fixed and paraffin-embedded clinical specimens on the prostate tissue microarray were obtained from the archive of the Institute for Pathology, University Hospital Basel, Switzerland. The tissue microarray was constructed according to the method previously described [182]. The diameter of each tissue spot was 0.6mm. Specimens were kept anonymous, and the experiments were performed according to the guidelines of the ethical committee of the University of Basel.

10q22 tissue microarray (TMA)

This is a TMA for screening 10q22 amplification. It contains 9 human samples derived from with advanced PCa that are characterised by an amplified signal using a probe for the gene vinculin (pers. Commun. W.Fu) and 6 controls. Each of these cases was represented in four replicates in order to covering a greater area and thereby allowing a better overview over the tumour. In addition there were two replicates of the cell lines PC-3, LNCaP, BPH-1, CWR22R, and JCA-1, each. The samples were recruited from archives of formalin fixed tissue of human biopsies and autopsies.

Bacteria

Bacteria strains were obtained from the Sanger Institute (Cambridge, UK). They belong to the RP-11 strains harbouring bacterial artificial chromosomes (BAC) from human genetic material with the exception of the BC RP13-39P13. The bacteria were plated for single colony and then the presence of the correct BAC was verified by PCR analysis of STS sequences present in the BAC. They were grown in low broth (LB) that contained 20 µg/ml chloramphenicol as selective marker. For solid media 1% agarose was added to the LB

medium. Bacteria were grown at 37°C except for BAC extraction. For extraction of DNA they were grown at room temperature to increase yield of BAC DNA. Bacs used in this study: RP11-464F9, RP11-296D9, RP11-312P12, RP11-399K21, RP11-162M1, RP11-325D15, RP11-428P16, RP13-39p12, RP11-6P10, RP11-202P11, RP11-342M3, RP11-506M13, RP11-182L21, RP11-137H2, RP11-459P11 All of these BAC provide resistance to the antibiotic chloramphenicol.

LB is 10g Tryptone, 5g Yeast extract, 10g NaCl in 1l H_20. Before use this growth medium was sterilised by autoclaving.

Extraction of BAC DNA:

The bacteria were grown for one day at room temperature. Then 2 ml bacteria culture were collected by centrifugation. The pellet was resuspended in GTE (50 mM Glucose, 25 mM TRIS, and 10mM EDTA in H_2O) and lysed by addition of 1%SDS and 0.2N NaOH. The highly viscous solution was intensively mixed by pipetting in order to achieve complete lysis of the bacteria. Then protein was precipitated by addition of 7.5M Ammonium acetate (NH_4Ac). After 5min incubation at room temperature insoluble material was precipitated by centrifugation at maximal speed. The DNA was precipitated from the supernatant by addition of isopropanol and centrifugation. The DNA pellet was resuspended in 2M NH_3Ac, which allows removal of residual protein by centrifugation. The DNA was precipitated from the supernatant by addition of 1x volume isopropanol. Then it was resuspended in 50 µl H2O. Then 2µl RNAseA was added to degrade RNA in the DNA preparation.

DNA concentration was measured in a Nanodrop Spectrophotometer measuring absorption at 280nm

Digoxigenin labelling

1µg of purified plasmid DNA was labelled using a modified commercial nick translation kit (BioNick kit, Invitrogen). Instead of biotin (provided with the kit), digoxigenin was used as a

label to fit the needs of our established fluorescence detection system. In brief, the provided biotin nucleotide solution was replaced by a self-made nucleotide solution containing, 0.2 mM each dCTP, dGTP, dTTP 0.1 mM dATP, 500 mM Tris-HCl (pH 7.8), 50 mM MgCl2, 100 mM mercaptoethanol, and 100 µg/ml nuclease-free BSA. In a total reaction volume of 48µl 5 µl Enzyme mix (BioNick kit) 5 µl Nucleotide solution, 1µl Digoxigenin (Roche), 1µl DNA Polymerase1 (Invitrogen), and 1 µg DNA were mixed. Nick translation was performed at 16°C for 90 min. Then the labelled KCNMA1 probe was precipitated by addition of 0.1x volume sodium acetate and 2x volume ethanol, and dissolved in 50 µl H20.

Fluorescence in situ hybridisation (FISH)

Paraffin removal (3x5min in Xylol followed by 2x2min Ethanol 95% and air-drying) and enzymatic tissue pre-treatment (Vysis pre-treatment solution, 80°C, 15 min) of tissue sections mounted on glass slides was performed in a VP2000 Processor device (Vysis). Slides were rinsed in water for 2 min, incubated in protease K solution (Vysis) at 37°C for 70min, and rinsed in water again. Subsequently, slides were dehydrated in an ascending ethanol series (70%, 80%, and 95%) and air-dried.

A premixed hybridization cocktail containing 0.5 µl centromere 10 probe (CEP 10 Spectrum orange labelled; Vysis), 1.5 µl KCNMA1 probe (digoxigenin labelled), 1 µl Cot DNA (Invitrogen), and 7µl hybridization buffer (Vysis) was added to each slide. Slides were covered with cover slips and sealed with rubber cement (Starkey, La Grange, Illinois). For probe and target DNA denaturation, slides were heated to 72°C for 10 min. Probe and target DNA were allowed to hybridize overnight at 37°C.

The next day, slides was washed to a stringency of 2xSSC, 0.3%NP40, pH= 7-7.5 at 72°C for 2 min. The KCNMA1 probe was detected using the Dig detection kit (Roche) in a three-step immune reaction with a FITC coupled antibody as suggested by the manufacturer.

Specificity of the probe was tested on a human metaphase preparation. A probe was considered as specific when a co-localisation with a control probe that is specific to the centromere of chromosome 10 (CEP 10, Vysis) was observed. See **Fig 2a** for the BAC RP11-428P16. All FISH probes used during this study were verified the same way (data not shown). In the case of amplicon screening (**Fig 1B**) 25 cells randomly selected cells were counted per tumour. For analysis of prevalence of 10q22 amplification the most prevalent amplification ratio was estimated in tumour cells. A case was considered amplified if the amplification ratio is >2. The amplification ratio is defined as number of probe signals versus number of centromere signals.

4.2 Cell Culture and Analysis of BK channel modulation by Iberiotoxin and 17β-Estradiol

Cell culture

In routine cell culture all cell lines were grown in OPTI-MEM+ 10%FCS in vented flasks ($75cm^2$, Falcon). The cells were split in a ratio of 1:5-1:10 when they were confluent. The cells were detached by incubation in a ready to use solution of 1:1000 Trypsin-EDTA (Amimed) for 5-15 min

PC-3

PC-3 was derived from a lumbar vertebral metastasis of a 62 year old white man in 1979[217]. It is highly progressed, for example it neither expresses AR nor PSA[218]and is highly tumourigenic forming tumours in nude mice at 100% frequency. Literature reports an approximate doubling time of 33 h[218]. I found a doubling time of <24h which might be due to high serum concentration or differences in medium formulation, but adaptation to in vitro cell culture due to high passage number is likely. It grows as single cells with no tendency to aggregate. It adheres readily to plastic surfaces of culture bottles and even to uncoated glass surfaces. It is easily detached by brief trypsinisation in 5-10 minutes.

LNCaP

LNCaP cells were isolated from a needle aspiration biopsy of a lymph node metastasis from a 50 year old white man[219]. These cells tend to adhere loosely to surfaces and may be easily detached[220]. LNCaP detaches as sheets or cell aggregates in culture at high cell density. The same phenomenon happens upon trypsinisation making counting difficult or unreliable. In order to circumvent this problem LNCaP was washed with Trypsin solution once before trypsinisation, which was 10-15 min. Then the remaining cell clumps were ripped by vigorous pipetting. If a highly reliable cell count was required, clumps of cells were removed by filtration through a cell strainer (Falcon). In our experimental condition, the doubling time was less than 24 h. Literature reports a doubling time of 2 days [218,220]. This might be due to different media and high amount of FCS present. Another explanation is that the LNCaP strain used in this study has a relatively long history of culture and has already adapted to in vitro culture conditions. In an assay that achieved androgen independent growth of LNCaP, cells with high passage number showed increased number of genetic changes including microsatelite instability and allelic loss [221]. These increased genetic alterations may be associated with the development of the androgen-unresponsive phenotype. Similar mechanisms may be involved in acceleration of growth that I observed in contrast to literature. As a consequence the cell line used in this study named LNCaP may have a significantly different genotype compared to the originally described cell lines. Thus repeating these experiments with other LNCaP strains with well-known passage number and genotype may yield different growth rates than reported here.

BPH-1

BPH-1 was derived from a 68 year old patient undergoing transurethral resection of the prostate (TURP) to help clear urinary obstruction consistent with BPH. The donor had not undergone any hormonal therapy and did not have malignant disease [222]. The cells were

maintained in culture for 11 days and then immortalised with a virus carrying the SV40 T antigen and selected for resistance to geneticin.

The cells grow as solid monolayer of a typical epithelial phenotype. This cell line does not form tumours in nude mice, although small clumps of cells were recovered from the graft sites indicating that cells survived in the host animals[223].

Growth experiments with Iberiotoxin and 17 β-Estradiol

For the proliferation assays, 25'000 cells were plated per well of a 6-well plate (Falcon) in 3ml OPTI-MEM+10% FCS. The medium was changed to 3ml OPTI-MEM+1% FCS after 1 day of growth. At day 2 after seeding the medium was changed to OPTI-MEM+ 0.4%Albumax (Invitrogen) containing the agent of interest. In addition the solvents, PBS or ethanol, respectively, were added to achieve comparable results. Iberiotoxin was diluted in PBS and used at a final concentration of 20 nM. 17 b-Estradiol (Sigma) was diluted in 70% ethanol and used at a final concentration of 1 nM

After two days of growth the cells were detached and total cell number was counted in a Neubauer chamber. Then the virtual growth rate k form the equation $A_{(t=2)}=A_{(t=0)}e^{kt}$ was calculated. $A_{(t=0)}$ is cell number at day 0, when estradiol and iberiotoxin were added. $A_{(t=2)}$ is the cell number at day 2. t is time in days.

4.3 PCR and Analysis of mRNA Expression

PCR

PCR Primers were designed using net-based primer3 software (http://frodo.wi.mit.edu/cgi-bin/primer3/primer3_www.cgi) generating primer with a predicted annealing temperature of 53-61°C using the TMUtility.1.5 software (http://www.idahotech.com/downloads_up/ index.html) for prediction of the annealing temperature using the LightCycler Fast Start DNA Master Sybr Green kit (Roche Molecular Diagnostics) with primer concentration of 50 µM and 2mM Mg^{2+}. For gene expression analysis using LightCycler technology the PCR primers

were selected to generate 100-300 bp amplification products (See Table 2). Whenever possible these products were selected to span at least one exon/ intron boundary as predicted by ensembl (www.ensembl.org) to reduce the effect of contamination by genomic material due to incomplete DNA digestion during RNA extraction. For LightCycler analysis of gene expression the LightCycler Fast Start DNA Master Sybr Green kit (Roche molecular Diagnostics) was used following the suppliers suggestions.

Routinely conventional PCR was performed using 0.4 µl Taq Polymerase (Qiagen), 2 µl dNTP (2.5 nM) each and 1 µl both forward and reverse Primer (10 µM). The template was added in a reasonable low concentration. Water was added to 20 µl.

For colony PCR the template was added without performing DNA purification by directly streaking very little material of the clone of interest (e.g. a given E.coli strain) into the PCR tube. Then the prepared PCR master mix was added and the reaction immediately started.

The routine PCR protocol was an initial step at 95°C for 3 min. Then the PCR cycles were: melting at 95°C 30 sec, annealing 52-59°C 30 sec, DNA synthesis at 72°C 1min. 25-40 PCR cycles. Then the product was cooled to 4°C.

PCR Primers:

See table 'PCR primers, genes'

Gel electrophoresis

Standard agarose gels contained 1% agarose in 1x TAE Buffer and 4 µl Ethidiumbromide per 100ml gel. Running buffer was TAE. DNA or RNA samples were mixed with Blue Juice usually in a ratio of 4:1 for PCR and 1:1 for extracted DNA or RNA. Then 10 µl were loaded and the gel was run for 15min- 30min at a constant voltage of 60-120V, respectively. 1x TAE was prepared from a 50x TAE stock. 50x TAE stock is 242g TRISbase, 57.1 ml acetic acid, 100ml 0.5M EDTA pH=8.0 in a total volume of 1l.

RNA extraction

The material (cell lines or frozen genomic material) was lysed by addition of Trizol (Invitrogen). Lysis was improved by vigorous shaking. 0.2ml of chloroform was added per 1ml of Trizol. After mixing by vigorous shaking the lysates was incubate at room temperature for 2-3 min. Then it was centrifuged at maximally 12'000g for 15 min at 4°C. The aqueous upper phase containing the RNA was transferred into a new tube. Then 0.5 ml of isopropanol was added per 1ml of Trizol initially used. The samples were incubated at room temperature for 15 min, which was followed by centrifugation at maximally 12'000g for 15 min at 4°C. Then RNA pellet was dissolved in the RLT buffer of the RNAeasy minikit. The supplied protocol of the RNA minikit was followed without modification including the optional DNA digestion. This protocol was followed because Trizol is more potent in lysis (especially in the case of tumour biopsy material) and the on column protocol of the RNAeasy minikit allows efficient removal of genomic DNA and avoids contamination with DNAse (pers. Comm. Dr. K. Struckmann).

For analysis of siRNA efficiency, the unmodified RNAeasy kit including the optional DNA on column digestion step was used. In this case the provided RLT buffer of the RNAeasy minikit conveniently achieves lysis of the cells in the culture vial. Thus there is no need to perform the more complicated protocol described above.

Extracted RNA was stored for short terms in the provided RNAse free water (RNAeasy mini kit) at -20°C.

cDNA synthesis

For cDNA synthesis the superscript II cDNA synthesis kit (Invitrogen) was used according to the manufacturer's instructions. Preferentially 1 µg total RNA was transcribed. For LightCycler analysis of gene expression this cDNA solution was diluted 1:50 using 5 µl per reaction.

Oligo dT were used as primers for the cDNA synthesis excepted from the RNA extracted from human prostate cancer biopsy that was transcribed with random hexamers.

4.4 siRNA and Western blotting

siRNA

siRNA design: In order to avoid problems with target sequence selection we chose a Qiagen offer to design and synthesise custom siRNA (k1:gactggcagagtcctggttgt, k2: gtgggtctgtccttccctact, k3: gaccgtcctgagtggccatgt, k4: acgcccttagaggtggctaca). In addition we ordered control (non-silencing) siRNA (Qiagen #1022076) and fluorescent-labelled control (non-silencing) siRNA, Rhodamine (Qiagen #1022083) as random sequence inactive siRNA controls. The lyophilised siRNA was solved in the provided siRNA buffer (100mM KOAc, 30mM HEPES KOH, 2mM MgOAc, pH=7.4, 1min 90°C, 1h 37°C, and stored for daily use at –20°C)

-Transfection: For transfection we chose Lipofectamine 2000 (Invitrogen, #11668-027) as best suited transfection agent for our cell line PC3 out of the selection Lipofectamine 2000, Oligofectamine (Invitrogen, #12252-011), siPORT™ *Amine* (Ambion, #4502), and siPORT™ *Lipid* (Ambion, #4504). For transfection we basically followed suppliers instructions taking care not to mix the transfection agents too intense, which could destroy the formed transfection complexes. 50'000 cells were seeded into one well of a 6-well BD Falcon™ Cell Culture Plate (Becton-Dickinson, #353046) one day before transfection in 3 ml OPTI-MEM (Gibco, 31985-047) containing 10% FCS (Amimed, 2-01F00-I). When transfecting cells no antibiotics were used to avoid toxic effects of these compounds in combination to the transfection agents (see product descriptions). For transfection 5 µl of siRNA stock solution (20nM) was added to 250 µl OPTI-MEM and vortexed. Then 5 µl Lipofectamine2000 was added to 250 µl OPTI-MEM and mixed by simply inverting the tube. After 5 min incubation the two solutions were combined, carefully mixed and incubated for 20 min. The cells were

washed once with Optimem. Then 2.5 ml OPTI-MEM was applied and the 0.5ml transfection complex solution was added onto the cells and carefully mixed by rocking the dish back and forth. After 4h of incubation the medium was changed to 3 ml OPTI-MEM with 10% FCS washing away the transfection medium.

Western blotting:

For western blotting, cells were grown in 6-well plates (Falcon). The cells were lysed by addition of 150-200 µl lysis buffer (list see below) and the lysat was transferred into 1.5ml Eppendorf tubes. Solid fragments were removed by centrifugation. The lysates were stored at -20°C.

Protein concentration:

Was measured using the Bio-Rad Protein Assay Dye Reagent Concentrate (BioRad) following the manufacturer's instructions.

Lysis buffers:

2%SDS

50mM TRIS CL (pH 6.8), 2% SDS, 10% Glycerol

This buffer may be prepared and stored at room temperature. Add 100mM dithiotreitol (DTT) before use. This buffer may be used as loading buffer. In this case double the concentration of all components and add 0.2% bromophenol blue.

1% Triton

Triton-X100 10 mM Tris, pH 7.4 Extract Buffer:

100 mM NaCl, 1 mM EDTA, 1 mM EGTA, 1 mM NaF, 20 mM Na4P2O7, 2 mM Na3VO4, 1% Triton X-100, 10% glycerol, 0.1% SDS, 0.5% deoxycholate, 1 mM PMSF, 0.5% Triton-buffer

CSK

0.5% Triton-X100, 100mM NaCl, 300mM Sucrose, 10mM sodium phosphate, 10% Glycerol, p=6.8

add prior to use from fresh stock:

2µg/ml Leupeptin, 1mM PMSF, 10mM NaF, 2.5 mM Na3VO4, 5 µl/ml protease inhibitor mix (Sigma)

PMSF is unstable and must be added prior to use, even if added previously.

This buffer also contains phosphatase inhibitors and may be used for preparation of phosphorylated protein.

To the 2% SDS and Triton X100 Lysis buffers 1 tablet of complete mini protease inhibitor (Roche) per 10 ml of lysis buffer was added just before use.

BK channel antibodies: APC 107 (Alomone labs); MaxiK-a, rabbit polyclonal (Affinity Bioreagents); Maxi Potassium channel alpha antibody (Abcam); anti-tubulin (bovine), mouse IgG1, monoclonal (Molecular Probes), Mouse monoclonal (6C5) to GPDH (Abcam)

Horse radish peroxidase coupled goat anti rabbit (Jackson Immuno Research Laboratories); Horse radish peroxidase coupled goat anti mouse (Jackson Immuno Research Laboratories)

Sodium dodecylsulfate polyacrylamid gel electrophoresis (SDS PAGE)

Antibodies were validated in a self prepared 6% acrylamin/bisacrylamid gel [224]. 5ml gel contained 2.6ml H_2O, 1ml 30% Acrylamid Mix (supplier), 1.5ml Tris pH=8.8, 0.05 ml 10% SDS, 0.05 ml ammonium persulfate, 4 µl TEMED. On top of this resolving gel was a 5% stacking gel. 1 ml of this stacking gel contained: 0.68 ml H_2O, 0.17 ml 30% Acrylamid Mix (supplier), 0.13 ml Tris pH=6.8, 0.01 ml 10% SDS, 0.01 ml ammonium persulfate, 1 µl TEMED.

Loading, running of the gel, and transfer to PVDF membrane were performed as described by Sambrook et al. [224]

For analysis of BK channel protein knockdown in response to siRNA, precast NuPAGE Novex 4-12% Bis-Tris gels (Invitrogen) were used. The supplied protocol was followed for preparing of the samples, running of the gel, and transfer to a PVDF membrane.

The Colour Markers, High Range, (M.W. 29,000-205,000) was used as molecular weight marker (Sigma, C 3312)

Hybridisation of antibodies:

After transfer the PVDF membrane was blocked by incubation in phosphate buffered saline (PBS), 0.05% Tween, 4% dry milk for 15 min at RT. Then the blocking buffer was washed of with PBS and the 1° antibody was incubated. It was diluted in PBS, 0.05% Tween, 0.4% BSA. The membrane was washed 3 times in PBS, 0.05% Tween for at least 15 min. Then the secondary HRPT coupled antibody was incubated. It was diluted in PBS, 0.05% Tween, 4% dry milk. Then the membrane was washed 3 times in PBS, 0.05% Tween for at least 15 min.

The antibody staining was detected using the ECL Plus™ Western Blotting Detection Reagents (Amersham Biosciences) was used. The membrane was exposed to a Kodak X-Omat Film to detect cheminoluminescence. Exposure times were 2-3 min for the anti-tubulin 1° antibody and >15 min for anti BK channel antibodies. The films were developed in a Curix table-top processor (AGFA).

Table 2: 'PCR primers'

Primer Pair	Forward sequence	Reverse sequence	Length of product
Calcineurin1	GACATCCATGGCCAATTTTT	TTCATGGTTGCCTCTCAGAA	
Calcineurin2	CTGACTCCCACAGGGATGTT	TGCGGTGTTCAGAGAATTGA	
Anx71	GCTGCCAACTTCGATGCTAT	AGAGGGCCAGGATCAGTTCT	
Anx72	CTTGCCACAAGAAGCTTTCC	TGTGCCAGCACCTTTCA	
Plau1	ACTCCAAAGGCAGCAATGAA	GGCCTTTCCTCGGTAAAAGT	
Plau2	GTCACCACCAAAATGCTGTG	GCGGATCCAGGGTAAGAAGT	
Kcnma11	ATATCCGCCCAGACACTGAC	ATCGTTGGCTGCAATAAACC	
KCNMA12	TTGGACCAAGACGATGATGA	CCTCTAAGGGCGTTTTCCTC	
DLG51	CTGTGGGAGACAGGATCGTT	GGCTCGAAAACTCAGCATCT	
DLG52	CATCTGTCATCGACCCACTG	GCAGGACTGTCATCCTCCAC	
MYST41	AAAGGGGCACCTCAGTATCC	GGATGGGTGTCCACTACTGC	
MYST42	AAGCTCTTCCTGGACCACAA	TGAGAAACCGTCCAAATCCT	
GPDH	GAAATCCCATCACCATCTTCC	CAGAGATGATGACCCTTTTGG	

5. References

1. Hsing, A. W., Tsao, L. & Devesa, S. S. International trends and patterns of prostate cancer incidence and mortality. *Int J Cancer* **85**, 60-7 (2000).
2. Zaridze, D. G. & Boyle, P. Cancer of the prostate: epidemiology and aetiology. *Br J Urol* **59**, 493-502 (1987).
3. Dhom, G. Epidemiologic aspects of latent and clinically manifest carcinoma of the prostate. *J Cancer Res Clin Oncol* **106**, 210-8 (1983).
4. Sakr, W. A. et al. Age and racial distribution of prostatic intraepithelial neoplasia. *Eur Urol* **30**, 138-44 (1996).
5. Dijkman, G. A. & Debruyne, F. M. Epidemiology of prostate cancer. *Eur Urol* **30**, 281-95 (1996).
6. Waterbor, J. W. & Bueschen, A. J. Prostate cancer screening (United States). *Cancer Causes Control* **6**, 267-74 (1995).
7. Klotz, L. Active surveillance for prostate cancer: for whom? *J Clin Oncol* **23**, 8165-9 (2005).
8. Cooperberg, M. R., Moul, J. W. & Carroll, P. R. The changing face of prostate cancer. *J Clin Oncol* **23**, 8146-51 (2005).
9. Bostwick, D. G. et al. Human prostate cancer risk factors. *Cancer* **101**, 2371-490 (2004).
10. Gronberg, H., Wiklund, F. & Damber, J. E. Age specific risks of familial prostate carcinoma: a basis for screening recommendations in high risk populations. *Cancer* **86**, 477-83 (1999).
11. Cotter, M. P., Gern, R. W., Ho, G. Y., Chang, R. Y. & Burk, R. D. Role of family history and ethnicity on the mode and age of prostate cancer presentation. *Prostate* **50**, 216-21 (2002).
12. Kolonel, L. N., Altshuler, D. & Henderson, B. E. The multiethnic cohort study: exploring genes, lifestyle and cancer risk. *Nat Rev Cancer* **4**, 519-27 (2004).
13. Whittemore, A. S. et al. Prostate cancer in relation to diet, physical activity, and body size in blacks, whites, and Asians in the United States and Canada. *J Natl Cancer Inst* **87**, 652-61 (1995).
14. Pienta, K. J., Goodson, J. A. & Esper, P. S. Epidemiology of prostate cancer: molecular and environmental clues. *Urology* **48**, 676-83 (1996).
15. Fraser, M. L., Lee, A. H. & Binns, C. W. Lycopene and prostate cancer: emerging evidence. *Expert Rev Anticancer Ther* **5**, 847-54 (2005).
16. Bostwick, D. G. Prospective origins of prostate carcinoma. Prostatic intraepithelial neoplasia and atypical adenomatous hyperplasia. *Cancer* **78**, 330-6 (1996).
17. Nagle, R. B., Brawer, M. K., Kittelson, J. & Clark, V. Phenotypic relationships of prostatic intraepithelial neoplasia to invasive prostatic carcinoma. *Am J Pathol* **138**, 119-28 (1991).
18. Xue, Y., Smedts, F., Debruyne, F. M., de la Rosette, J. J. & Schalken, J. A. Identification of intermediate cell types by keratin expression in the developing human prostate. *Prostate* **34**, 292-301 (1998).
19. Wernert, N., Seitz, G. & Achtstatter, T. Immunohistochemical investigation of different cytokeratins and vimentin in the prostate from the fetal period up to adulthood and in prostate carcinoma. *Pathol Res Pract* **182**, 617-26 (1987).
20. Foster, C. S. & Ke, Y. Stem cells in prostatic epithelia. *Int J Exp Pathol* **78**, 311-29 (1997).
21. Bonkhoff, H. Role of the basal cells in premalignant changes of the human prostate: a stem cell concept for the development of prostate cancer. *Eur Urol* **30**, 201-5 (1996).

22. Bonkhoff, H. & Remberger, K. Morphogenetic concepts of normal and abnormal growth in the human prostate. *Virchows Arch* **433**, 195-202 (1998).
23. Bonkhoff, H. & Remberger, K. Differentiation pathways and histogenetic aspects of normal and abnormal prostatic growth: a stem cell model. *Prostate* **28**, 98-106 (1996).
24. Foster, C. S. et al. Cellular and molecular pathology of prostate cancer precursors. *Scand J Urol Nephrol Suppl*, 19-43 (2000).
25. Montironi, R., Magi-Galluzzi, C. & Fabris, G. Apoptotic bodies in prostatic intraepithelial neoplasia and prostatic adenocarcinoma following total androgen ablation. *Pathol Res Pract* **191**, 873-80 (1995).
26. Evans, G. S. & Chandler, J. A. Cell proliferation studies in the rat prostate: II. The effects of castration and androgen-induced regeneration upon basal and secretory cell proliferation. *Prostate* **11**, 339-51 (1987).
27. Harkonen, P. L. & Makela, S. I. Role of estrogens in development of prostate cancer. *J Steroid Biochem Mol Biol* **92**, 297-305 (2004).
28. Chodak, G. W. Endocrine treatment of prostatic cancer. *Urology* **23**, 224-5 (1984).
29. Fong, Y. K., Milani, S. & Djavan, B. Natural history and clinical predictors of clinical progression in benign prostatic hyperplasia. *Curr Opin Urol* **15**, 35-8 (2005).
30. McNeal, J. E. Origin and development of carcinoma in the prostate. *Cancer* **23**, 24-34 (1969).
31. Bostwick, D. G. Progression of prostatic intraepithelial neoplasia to early invasive adenocarcinoma. *Eur Urol* **30**, 145-52 (1996).
32. Haggman, M. J., Macoska, J. A., Wojno, K. J. & Oesterling, J. E. The relationship between prostatic intraepithelial neoplasia and prostate cancer: critical issues. *J Urol* **158**, 12-22 (1997).
33. Bostwick, D. G., Pacelli, A. & Lopez-Beltran, A. Molecular biology of prostatic intraepithelial neoplasia. *Prostate* **29**, 117-34 (1996).
34. Humphrey, P. A. Gleason grading and prognostic factors in carcinoma of the prostate. *Mod Pathol* **17**, 292-306 (2004).
35. Bubendorf, L. et al. Metastatic patterns of prostate cancer: an autopsy study of 1,589 patients. *Hum Pathol* **31**, 578-83 (2000).
36. Mettlin, C. J., Murphy, G. P., Rosenthal, D. S. & Menck, H. R. The National Cancer Data Base report on prostate carcinoma after the peak in incidence rates in the U.S. The American College of Surgeons Commission on Cancer and the American Cancer Society. *Cancer* **83**, 1679-84 (1998).
37. Shekarriz, B. et al. Impact of preoperative serum PSA level from 0 to 10 ng/ml on pathological findings and disease-free survival after radical prostatectomy. *Prostate* **48**, 136-43. (2001).
38. Damber, J. E. Decreasing mortality rates for prostate cancer: possible role of hormonal therapy? *BJU Int* **93**, 695-701 (2004).
39. Partin, A. W. et al. The use of prostate specific antigen, clinical stage and Gleason score to predict pathological stage in men with localized prostate cancer. *J Urol* **150**, 110-114 (1993).
40. Kattan, M. W., Stapleton, A. M., Wheeler, T. M. & Scardino, P. T. Evaluation of a nomogram used to predict the pathologic stage of clinically localized prostate carcinoma. *Cancer* **79**, 528-537 (1997).
41. Gronau, E., Goppelt, M., Harzmann, R. & Weckermann, D. Prostate cancer relapse after therapy with curative intention: a diagnostic and therapeutic dilemma. *Onkologie* **28**, 361-6 (2005).
42. Kirby, R. S., Christmas, T. J. & Brawer, M. in *Prostat cancer* 93-112 (Times Mirror International Publishers, London, 1996).

43. Westin, P., Stattin, P., Damber, J. E. & Bergh, A. Castration therapy rapidly induces apoptosis in a minority and decreases cell proliferation in a majority of human prostatic tumors. *Am J Pathol* **146**, 1368-75 (1995).
44. Miyamoto, H., Messing, E. M. & Chang, C. Androgen deprivation therapy for prostate cancer: current status and future prospects. *Prostate* **61**, 332-53 (2004).
45. Scher, H. I., Mazumdar, M. & Kelly, W. K. Clinical trials in relapsed prostate cancer: defining the target. *J Natl Cancer Inst* **88**, 1623-34 (1996).
46. Tannock, I. F. et al. Docetaxel plus prednisone or mitoxantrone plus prednisone for advanced prostate cancer. *N Engl J Med* **351**, 1502-12 (2004).
47. Petrylak, D. P. et al. Docetaxel and estramustine compared with mitoxantrone and prednisone for advanced refractory prostate cancer. *N Engl J Med* **351**, 1513-20 (2004).
48. Scher, H. I. & Sawyers, C. L. Biology of progressive, castration-resistant prostate cancer: directed therapies targeting the androgen-receptor signaling axis. *J Clin Oncol* **23**, 8253-61 (2005).
49. Taplin, M. E. & Balk, S. P. Androgen receptor: a key molecule in the progression of prostate cancer to hormone independence. *J Cell Biochem* **91**, 483-90 (2004).
50. Visakorpi, T. et al. In vivo amplification of the androgen receptor gene and progression of human prostate cancer. *Nat Genet* **9**, 401-6 (1995).
51. Taplin, M. E. et al. Selection for androgen receptor mutations in prostate cancers treated with androgen antagonist. *Cancer Res* **59**, 2511-5 (1999).
52. Feldman, B. J. & Feldman, D. The development of androgen-independent prostate cancer. *Nat Rev Cancer* **1**, 34-45 (2001).
53. Balk, S. P. Androgen receptor as a target in androgen-independent prostate cancer. *Urology* **60**, 132-8; discussion 138-9 (2002).
54. Wen, Y. et al. HER-2/neu promotes androgen-independent survival and growth of prostate cancer cells through the Akt pathway. *Cancer Res* **60**, 6841-5 (2000).
55. Culig, Z. et al. Androgen receptor activation in prostatic tumor cell lines by insulin-like growth factor-I, keratinocyte growth factor, and epidermal growth factor. *Cancer Res* **54**, 5474-8 (1994).
56. Russell, P. J., Bennett, S. & Stricker, P. Growth factor involvement in progression of prostate cancer. *Clin Chem* **44**, 705-23 (1998).
57. Abreu-Martin, M. T., Chari, A., Palladino, A. A., Craft, N. A. & Sawyers, C. L. Mitogen-activated protein kinase kinase kinase 1 activates androgen receptor-dependent transcription and apoptosis in prostate cancer. *Mol Cell Biol* **19**, 5143-54 (1999).
58. Li, P., Nicosia, S. V. & Bai, W. Antagonism between PTEN/MMAC1/TEP-1 and androgen receptor in growth and apoptosis of prostatic cancer cells. *J Biol Chem* **276**, 20444-50 (2001).
59. Kwabi-Addo, B. et al. Haploinsufficiency of the Pten tumor suppressor gene promotes prostate cancer progression. *Proc Natl Acad Sci U S A* **98**, 11563-8 (2001).
60. Smith, P. C., Hobisch, A., Lin, D. L., Culig, Z. & Keller, E. T. Interleukin-6 and prostate cancer progression. *Cytokine Growth Factor Rev* **12**, 33-40 (2001).
61. Culig, Z. et al. Regulation of prostatic growth and function by peptide growth factors. *Prostate* **28**, 392-405 (1996).
62. Abrahamsson, P. A. Neuroendocrine cells in tumour growth of the prostate. *Endocr Relat Cancer* **6**, 503-19 (1999).
63. Meyer, H. A., Ahrens-Fath, I., Sommer, A. & Haendler, B. Novel molecular aspects of prostate carcinogenesis. *Biomed Pharmacother* **58**, 10-6 (2004).

64. Segal, N. H., Cohen, R. J., Haffejee, Z. & Savage, N. BCL-2 proto-oncogene expression in prostate cancer and its relationship to the prostatic neuroendocrine cell. *Arch Pathol Lab Med* **118**, 616-8 (1994).
65. Kallioniemi, A. et al. Comparative genomic hybridization for molecular cytogenetic analysis of solid tumors. *Science* **258**, 818-21 (1992).
66. Visakorpi, T. et al. Genetic changes in primary and recurrent prostate cancer by comparative genomic hybridization. *Cancer Res* **55**, 342-7 (1995).
67. Cher, M. L. et al. Comparative genomic hybridization, allelic imbalance, and fluorescence in situ hybridization on chromosome 8 in prostate cancer. *Genes Chromosomes Cancer* **11**, 153-62 (1994).
68. Joos, S. et al. Mapping of chromosomal gains and losses in prostate cancer by comparative genomic hybridization. *Genes Chromosomes Cancer* **14**, 267-76 (1995).
69. Nupponen, N. N., Hyytinen, E. R., Kallioniemi, A. H. & Visakorpi, T. Genetic alterations in prostate cancer cell lines detected by comparative genomic hybridization. *Cancer Genet Cytogenet* **101**, 53-7 (1998).
70. Nupponen, N. N., Kakkola, L., Koivisto, P. & Visakorpi, T. Genetic alterations in hormone-refractory recurrent prostate carcinomas. *Am J Pathol* **153**, 141-8 (1998).
71. Knuutila, S. et al. DNA copy number amplifications in human neoplasms: review of comparative genomic hybridization studies. *Am J Pathol* **152**, 1107-23 (1998).
72. Pegram, M. & Slamon, D. Biological rationale for HER2/neu (c-erbB2) as a target for monoclonal antibody therapy. *Semin Oncol* **27**, 13-9 (2000).
73. Koivisto, P. et al. Androgen receptor gene amplification: a possible molecular mechanism for androgen deprivation therapy failure in prostate cancer. *Cancer Res* **57**, 314-319 (1997).
74. Palmberg, C. et al. Androgen receptor gene amplification at primary progression predicts response to combined androgen blockade as second line therapy for advanced prostate cancer. *J Urol* **164**, 1992-5 (2000).
75. Jenkins, R. B., Qian, J., Lieber, M. M. & Bostwick, D. G. Detection of c-myc oncogene amplification and chromosomal anomalies in metastatic prostatic carcinoma by fluorescence in situ hybridization. *Cancer Res* **57**, 524-31 (1997).
76. Reiter, R. E. et al. Coamplification of prostate stem cell antigen (PSCA) and MYC in locally advanced prostate cancer. *Genes Chromosomes Cancer* **27**, 95-103 (2000).
77. Porkka, K. P., Tammela, T. L., Vessella, R. L. & Visakorpi, T. RAD21 and KIAA0196 at 8q24 are amplified and overexpressed in prostate cancer. *Genes Chromosomes Cancer* **39**, 1-10 (2004).
78. Nupponen, N. N. et al. Amplification and overexpression of p40 subunit of eukaryotic translation initiation factor 3 in breast and prostate cancer. *Am J Pathol* **154**, 1777-83 (1999).
79. Kaltz-Wittmer, C. et al. FISH analysis of gene aberrations (MYC, CCND1, ERBB2, RB, and AR) in advanced prostatic carcinomas before and after androgen deprivation therapy. *Lab Invest* **80**, 1455-64 (2000).
80. Latil, A. et al. Oncogene amplifications in early-stage human prostate carcinomas. *Int J Cancer* **59**, 637-8 (1994).
81. Sattler, H. P. et al. Novel amplification unit at chromosome 3q25-q27 in human prostate cancer. *Prostate* **45**, 207-15 (2000).
82. El Gedaily, A. et al. Discovery of new amplification loci in prostate cancer by comparative genomic hybridization. *Prostate* **46**, 184-190 (2001).
83. Lau, C. C. et al. Frequent amplification and rearrangement of chromosomal bands 6p12-p21 and 17p11.2 in osteosarcoma. *Genes Chromosomes Cancer* **39**, 11-21 (2004).

84. Hovey, R. M. et al. Genetic alterations in primary bladder cancers and their metastases. *Cancer Res* **58**, 3555-60 (1998).
85. Taguchi, T. et al. Combined chromosome microdissection and comparative genomic hybridization detect multiple sites of amplification DNA in a human lung carcinoma cell line. *Genes Chromosomes Cancer* **20**, 208-12 (1997).
86. Muleris, M., Almeida, A., Gerbault-Seureau, M., Malfoy, B. & Dutrillaux, B. Detection of DNA amplification in 17 primary breast carcinomas with homogeneously staining regions by a modified comparative genomic hybridization technique. *Genes Chromosomes Cancer* **10**, 160-70 (1994).
87. Leube, B. et al. Refined mapping of allele loss at chromosome 10q23-26 in prostate cancer. *Prostate* **50**, 135-44 (2002).
88. Bertino, J. R. et al. Gene amplification and altered enzymes as mechanisms for the development of drug resistance. *Cancer Treat Rep* **67**, 901-4 (1983).
89. Dworetzky, S. I., Trojnacki, J. T. & Gribkoff, V. K. Cloning and expression of a human large-conductance calcium-activated potassium channel. *Brain Res Mol Brain Res* **27**, 189-93 (1994).
90. Magleby, K. L. Gating mechanism of BK (Slo1) channels: so near, yet so far. *J Gen Physiol* **121**, 81-96 (2003).
91. Pallanck, L. & Ganetzky, B. Cloning and characterization of human and mouse homologs of the Drosophila calcium-activated potassium channel gene, slowpoke. *Hum Mol Genet* **3**, 1239-43 (1994).
92. Schmalhofer, W. A. et al. Role of the C-terminus of the high-conductance calcium-activated potassium channel in channel structure and function. *Biochemistry* **44**, 10135-44 (2005).
93. Wang, Y. W., Ding, J. P., Xia, X. M. & Lingle, C. J. Consequences of the stoichiometry of Slo1 alpha and auxiliary beta subunits on functional properties of large-conductance Ca2+-activated K+ channels. *J Neurosci* **22**, 1550-61 (2002).
94. Knaus, H. G., Garcia-Calvo, M., Kaczorowski, G. J. & Garcia, M. L. Subunit composition of the high conductance calcium-activated potassium channel from smooth muscle, a representative of the mSlo and slowpoke family of potassium channels. *J Biol Chem* **269**, 3921-4 (1994).
95. Wallner, M., Meera, P. & Toro, L. Molecular basis of fast inactivation in voltage and Ca2+-activated K+ channels: a transmembrane beta-subunit homolog. *Proc Natl Acad Sci U S A* **96**, 4137-42 (1999).
96. Riazi, M. A. et al. Identification of a putative regulatory subunit of a calcium-activated potassium channel in the dup(3q) syndrome region and a related sequence on 22q11.2. *Genomics* **62**, 90-4 (1999).
97. Behrens, R. et al. hKCNMB3 and hKCNMB4, cloning and characterization of two members of the large-conductance calcium-activated potassium channel beta subunit family. *FEBS Lett* **474**, 99-106 (2000).
98. Brenner, R., Jegla, T. J., Wickenden, A., Liu, Y. & Aldrich, R. W. Cloning and functional characterization of novel large conductance calcium-activated potassium channel beta subunits, hKCNMB3 and hKCNMB4. *J Biol Chem* **275**, 6453-61 (2000).
99. Garcia, M. L. et al. Use of toxins to study potassium channels. *J Bioenerg Biomembr* **23**, 615-46 (1991).
100. Dworetzky, S. I. et al. Phenotypic alteration of a human BK (hSlo) channel by hSlobeta subunit coexpression: changes in blocker sensitivity, activation/relaxation and inactivation kinetics, and protein kinase A modulation. *J Neurosci* **16**, 4543-50 (1996).

101. Meera, P., Wallner, M. & Toro, L. A neuronal beta subunit (KCNMB4) makes the large conductance, voltage- and Ca2+-activated K+ channel resistant to charybdotoxin and iberiotoxin. *Proc Natl Acad Sci U S A* **97**, 5562-7 (2000).
102. Valverde, M. A. et al. Acute activation of Maxi-K channels (hSlo) by estradiol binding to the beta subunit. *Science* **285**, 1929-31. (1999).
103. Tian, L. et al. Alternative splicing switches potassium channel sensitivity to protein phosphorylation. *J Biol Chem* **276**, 7717-20 (2001).
104. Chen, L. et al. Functionally Diverse Complement of Large Conductance Calcium- and Voltage-activated Potassium Channel (BK) {alpha}-Subunits Generated from a Single Site of Splicing. *J Biol Chem* **280**, 33599-609 (2005).
105. Weaver, A. K., Liu, X. & Sontheimer, H. Role for calcium-activated potassium channels (BK) in growth control of human malignant glioma cells. *J Neurosci Res* **78**, 224-34 (2004).
106. Ouadid-Ahidouch, H., Roudbaraki, M., Ahidouch, A., Delcourt, P. & Prevarskaya, N. Cell-cycle-dependent expression of the large Ca2+-activated K+ channels in breast cancer cells. *Biochem Biophys Res Commun* **316**, 244-51 (2004).
107. Kodal, H. et al. Involvement of calcium-activated potassium channels in the regulation of DNA synthesis in cultured Muller glial cells. *Invest Ophthalmol Vis Sci* **41**, 4262-7 (2000).
108. Song, M. et al. Hormonal control of protein expression and mRNA levels of the MaxiK channel alpha subunit in myometrium. *FEBS Lett* **460**, 427-32. (1999).
109. Tanaka, Y., Horinouchi, T., Tanaka, H., Shigenobu, K. & Koike, K. [BK channels play an important role as a negative feedback mechanism in the regulation of spontaneous rhythmic contraction of urinary bladder smooth muscles]. *Nippon Yakurigaku Zasshi* **120**, 106P-108P (2002).
110. Brayden, J. E. & Nelson, M. T. Regulation of arterial tone by activation of calcium-dependent potassium channels. *Science* **256**, 532-5. (1992).
111. Robitaille, R. & Charlton, M. P. Presynaptic calcium signals and transmitter release are modulated by calcium-activated potassium channels. *J Neurosci* **12**, 297-305. (1992).
112. Brandle, U. et al. Expression of Ca(2+)-activated K(+) channel subunits and splice variants in the rat cochlea. *Hear Res* **161**, 23-8 (2001).
113. Ruttiger, L. et al. Deletion of the Ca2+-activated potassium (BK) alpha-subunit but not the BKbeta1-subunit leads to progressive hearing loss. *Proc Natl Acad Sci U S A* **101**, 12922-7 (2004).
114. Blachly-Dyson, E., Baldini, A., Litt, M., McCabe, E. R. & Forte, M. Human genes encoding the voltage-dependent anion channel (VDAC) of the outer mitochondrial membrane: mapping and identification of two new isoforms. *Genomics* **20**, 62-7 (1994).
115. Cheng, E. H., Sheiko, T. V., Fisher, J. K., Craigen, W. J. & Korsmeyer, S. J. VDAC2 inhibits BAK activation and mitochondrial apoptosis. *Science* **301**, 513-7 (2003).
116. Janicke, F. et al. Urokinase (uPA) and its inhibitor PAI-1 are strong and independent prognostic factors in node-negative breast cancer. *Breast Cancer Res Treat* **24**, 195-208 (1993).
117. Duffy, M. J. & Duggan, C. The urokinase plasminogen activator system: a rich source of tumour markers for the individualised management of patients with cancer. *Clin Biochem* **37**, 541-8 (2004).
118. Liu, J. et al. Noncatalytic domain of uPA stimulates human extravillous trophoblast migration by using phospholipase C, phosphatidylinositol 3-kinase and mitogen-activated protein kinase. *Exp Cell Res* **286**, 138-51 (2003).

119. Helenius, M. A., Saramaki, O. R., Linja, M. J., Tammela, T. L. & Visakorpi, T. Amplification of urokinase gene in prostate cancer. *Cancer Res* **61**, 5340-4. (2001).
120. Arens, N., Gandhari, M., Bleyl, U. & Hildenbrand, R. In vitro suppression of urokinase plasminogen activator in breast cancer cells - A comparison of two antisense strategies. *Int J Oncol* **26**, 113-9 (2005).
121. Jankun, J., Keck, R. W., Skrzypczak-Jankun, E. & Swiercz, R. Inhibitors of urokinase reduce size of prostate cancer xenografts in severe combined immunodeficient mice. *Cancer Res* **57**, 559-63 (1997).
122. Sharma, M. et al. hZimp10 is an androgen receptor co-activator and forms a complex with SUMO-1 at replication foci. *Embo J* **22**, 6101-14 (2003).
123. Gloyn, A. L. et al. Human calcium/calmodulin-dependent protein kinase II gamma gene (CAMK2G): cloning, genomic structure and detection of variants in subjects with type II diabetes. *Diabetologia* **45**, 580-3 (2002).
124. Illario, M. et al. Calcium/calmodulin-dependent protein kinase II binds to Raf-1 and modulates integrin-stimulated ERK activation. *J Biol Chem* **278**, 45101-8 (2003).
125. Vitale, M., Di Matola, T., Fenzi, G., Illario, M. & Rossi, G. Fibronectin is required to prevent thyroid cell apoptosis through an integrin-mediated adhesion mechanism. *J Clin Endocrinol Metab* **83**, 3673-80 (1998).
126. Vitale, M. et al. Integrin binding to immobilized collagen and fibronectin stimulates the proliferation of human thyroid cells in culture. *Endocrinology* **138**, 1642-8 (1997).
127. Antoni, F. A. Mortyn Jones Memorial Lecture--1995. Calcium checks cyclic AMP--corticosteroid feedback in adenohypophysial corticotrophs. *J Neuroendocrinol* **8**, 659-72 (1996).
128. Wang, M. G., Yi, H., Guerini, D., Klee, C. B. & McBride, O. W. Calcineurin A alpha (PPP3CA), calcineurin A beta (PPP3CB) and calcineurin B (PPP3R1) are located on human chromosomes 4, 10q21-->q22 and 2p16-->p15 respectively. *Cytogenet Cell Genet* **72**, 236-41 (1996).
129. Aramburu, J., Heitman, J. & Crabtree, G. R. Calcineurin: a central controller of signalling in eukaryotes. *EMBO Rep* **5**, 343-8 (2004).
130. Lakshmikuttyamma, A., Selvakumar, P., Kanthan, R., Kanthan, S. C. & Sharma, R. K. Increased expression of calcineurin in human colorectal adenocarcinomas. *J Cell Biochem* **95**, 731-9 (2005).
131. Brook, N. R., Waller, J. R., Bicknell, G. R. & Nicholson, M. L. The novel antifibrotic agent pirfenidone attenuates the profibrotic environment generated by calcineurin inhibitors in the rat salt-depletion model. *Transplant Proc* **37**, 130-3 (2005).
132. Timmerman, L. A., Clipstone, N. A., Ho, S. N., Northrop, J. P. & Crabtree, G. R. Rapid shuttling of NF-AT in discrimination of Ca2+ signals and immunosuppression. *Nature* **383**, 837-40 (1996).
133. Dolmetsch, R. E., Lewis, R. S., Goodnow, C. C. & Healy, J. I. Differential activation of transcription factors induced by Ca2+ response amplitude and duration. *Nature* **386**, 855-8 (1997).
134. Champagne, N. et al. Identification of a Human Histone Acetyltransferase Related to Monocytic Leukemia Zinc Finger Protein. *J. Biol. Chem.* **274**, 28528-28536 (1999).
135. Pelletier, N., Champagne, N., Stifani, S. & Yang, X. J. MOZ and MORF histone acetyltransferases interact with the Runt-domain transcription factor Runx2. *Oncogene* **21**, 2729-40 (2002).
136. Burns, A. L. et al. Calcium channel activity of purified human synexin and structure of the human synexin gene. *Proc Natl Acad Sci U S A* **86**, 3798-802 (1989).
137. Caohuy, H., Srivastava, M. & Pollard, H. B. Membrane fusion protein synexin (annexin VII) as a Ca2+/GTP sensor in exocytotic secretion. *Proc Natl Acad Sci U S A* **93**, 10797-802 (1996).

138. Srivastava, M. et al. ANX7, a candidate tumor suppressor gene for prostate cancer. *Proc Natl Acad Sci U S A* **98**, 4575-80. (2001).
139. Srivastava, M. et al. Haploinsufficiency of Anx7 tumor suppressor gene and consequent genomic instability promotes tumorigenesis in the Anx7(+/-) mouse. *Proc Natl Acad Sci U S A* **100**, 14287-92 (2003).
140. Srivastava, M. et al. Prognostic impact of ANX7-GTPase in metastatic and HER2-negative breast cancer patients. *Clin Cancer Res* **10**, 2344-50 (2004).
141. Morimoto, S. et al. Saposin A: second cerebrosidase activator protein. *Proc Natl Acad Sci U S A* **86**, 3389-93 (1989).
142. Koochekpour, S. et al. Saposin C stimulates growth and invasion, activates p42/44 and SAPK/JNK signaling pathways of MAPK and upregulates uPA/uPAR expression in prostate cancer and stromal cells. *Asian J Androl* **7**, 147-58 (2005).
143. Koochekpour, S. et al. Amplification and overexpression of prosaposin in prostate cancer. *Genes Chromosomes Cancer* **44**, 351-64 (2005).
144. White, R. T. et al. Isolation and characterization of the human pulmonary surfactant apoprotein gene. *Nature* **317**, 361-3 (1985).
145. Katyal, S. L., Singh, G. & Locker, J. Characterization of a second human pulmonary surfactant-associated protein SP-A gene. *Am J Respir Cell Mol Biol* **6**, 446-52 (1992).
146. Ramet, M., Lofgren, J., Alho, O. P. & Hallman, M. Surfactant protein-A gene locus associated with recurrent otitis media. *J Pediatr* **138**, 266-8 (2001).
147. Selman, M. et al. Surfactant protein A and B genetic variants predispose to idiopathic pulmonary fibrosis. *Hum Genet* **113**, 542-50 (2003).
148. Haataja, R., Ramet, M., Marttila, R. & Hallman, M. Surfactant proteins A and B as interactive genetic determinants of neonatal respiratory distress syndrome. *Hum Mol Genet* **9**, 2751-60 (2000).
149. Sepehri, S. & Hernandez, N. The largest subunit of human RNA polymerase III is closely related to the largest subunit of yeast and trypanosome RNA polymerase III. *Genome Res* **7**, 1006-19 (1997).
150. Brown, S. J., Jewell, A., Maki, C. G. & Roufa, D. J. A cDNA encoding human ribosomal protein S24. *Gene* **91**, 293-6 (1990).
151. Xu, W. B. & Roufa, D. J. The gene encoding human ribosomal protein S24 and tissue-specific expression of differentially spliced mRNAs. *Gene* **169**, 257-62 (1996).
152. Nakamura, K., Shima, H., Watanabe, M., Haneji, T. & Kikuchi, K. Molecular cloning and characterization of a novel dual-specificity protein phosphatase possibly involved in spermatogenesis. *Biochem J* **344 Pt 3**, 819-25 (1999).
153. Chen, H. H., Luche, R., Wei, B. & Tonks, N. K. Characterization of two distinct dual specificity phosphatases encoded in alternative open reading frames of a single gene located on human chromosome 10q22.2. *J Biol Chem* **279**, 41404-13 (2004).
154. Spychala, J. et al. Cloning of human adenosine kinase cDNA: sequence similarity to microbial ribokinases and fructokinases. *Proc Natl Acad Sci U S A* **93**, 1232-7 (1996).
155. Nomura, N. et al. Prediction of the coding sequences of unidentified human genes. II. The coding sequences of 40 new genes (KIAA0041-KIAA0080) deduced by analysis of cDNA clones from human cell line KG-1. *DNA Res* **1**, 223-9 (1994).
156. Tani, K., Oyama, Y., Hatsuzawa, K. & Tagaya, M. Hypothetical protein KIAA0079 is a mammalian homologue of yeast Sec24p. *FEBS Lett* **447**, 247-50 (1999).
157. Humphries, D. E., Lanciotti, J. & Karlinsky, J. B. cDNA cloning, genomic organization and chromosomal localization of human heparan glucosaminyl N-deacetylase/N-sulphotransferase-2. *Biochem J* **332 (Pt 2)**, 303-7 (1998).
158. Humphries, D. E. et al. Heparin is essential for the storage of specific granule proteases in mast cells. *Nature* **400**, 769-72 (1999).

159. Forsberg, E. et al. Abnormal mast cells in mice deficient in a heparin-synthesizing enzyme. *Nature* **400**, 773-6 (1999).
160. Critchley, D. R. Cytoskeletal proteins talin and vinculin in integrin-mediated adhesion. *Biochem Soc Trans* **32**, 831-6 (2004).
161. Hazan, R. B., Kang, L., Roe, S., Borgen, P. I. & Rimm, D. L. Vinculin is associated with the E-cadherin adhesion complex. *J Biol Chem* **272**, 32448-53 (1997).
162. Subauste, M. C. et al. Vinculin modulation of paxillin-FAK interactions regulates ERK to control survival and motility. *J Cell Biol* **165**, 371-81 (2004).
163. Subauste, M. C., Nalbant, P., Adamson, E. D. & Hahn, K. M. Vinculin controls PTEN protein level by maintaining the interaction of the adherens junction protein beta-catenin with the scaffolding protein MAGI-2. *J Biol Chem* **280**, 5676-81 (2005).
164. Rodriguez Fernandez, J. L. et al. Suppression of tumorigenicity in transformed cells after transfection with vinculin cDNA. *J Cell Biol* **119**, 427-38. (1992).
165. Takada, F. et al. Myozenin: an alpha-actinin- and gamma-filamin-binding protein of skeletal muscle Z lines. *Proc Natl Acad Sci U S A* **98**, 1595-600 (2001).
166. Lawrence, J. G. Shared strategies in gene organization among prokaryotes and eukaryotes. *Cell* **110**, 407-13 (2002).
167. van Driel, R., Fransz, P. F. & Verschure, P. J. The eukaryotic genome: a system regulated at different hierarchical levels. *J Cell Sci* **116**, 4067-75 (2003).
168. van Bokhoven, A., Varella-Garcia, M., Korch, C. & Miller, G. J. TSU-Pr1 and JCA-1 cells are derivatives of T24 bladder carcinoma cells and are not of prostatic origin. *Cancer Res* **61**, 6340-4 (2001).
169. Liu, X., Chang, Y., Reinhart, P. H. & Sontheimer, H. Cloning and characterization of glioma BK, a novel BK channel isoform highly expressed in human glioma cells. *J Neurosci* **22**, 1840-9 (2002).
170. Olsen, M. L., Weaver, A. K., Ritch, P. S. & Sontheimer, H. Modulation of glioma BK channels via erbB2. *J Neurosci Res* (2005).
171. Albertson, D. G., Collins, C., McCormick, F. & Gray, J. W. Chromosome aberrations in solid tumors. *Nat Genet* **34**, 369-76 (2003).
172. Kallioniemi, O. P. et al. ERBB2 amplification in breast cancer analyzed by fluorescence in situ hybridization. *Proc Natl Acad Sci U S A* **89**, 5321-5 (1992).
173. Romond, E. H. et al. Trastuzumab plus adjuvant chemotherapy for operable HER2-positive breast cancer. *N Engl J Med* **353**, 1673-84 (2005).
174. DiGiovanna, M. P. et al. Active signaling by HER-2/neu in a subpopulation of HER-2/neu-overexpressing ductal carcinoma in situ: clinicopathological correlates. *Cancer Res* **62**, 6667-73 (2002).
175. Alimandi, M. et al. Cooperative signaling of ErbB3 and ErbB2 in neoplastic transformation and human mammary carcinomas. *Oncogene* **10**, 1813-21 (1995).
176. Bell, J. C. Oncogenes. *Cancer Lett* **40**, 1-5 (1988).
177. Saint-Ruf, C., Malfoy, B., Scholl, S., Zafrani, B. & Dutrillaux, B. GST pi gene is frequently coamplified with INT2 and HSTF1 proto-oncogenes in human breast cancers. *Oncogene* **6**, 403-6 (1991).
178. Walch, A. et al. Coamplification and coexpression of GRB7 and ERBB2 is found in high grade intraepithelial neoplasia and in invasive Barrett's carcinoma. *Int J Cancer* **112**, 747-53 (2004).
179. Reifenberger, G. et al. Refined mapping of 12q13-q15 amplicons in human malignant gliomas suggests CDK4/SAS and MDM2 as independent amplification targets. *Cancer Res* **56**, 5141-5 (1996).
180. Hui, A. B., Lo, K. W., Yin, X. L., Poon, W. S. & Ng, H. K. Detection of multiple gene amplifications in glioblastoma multiforme using array-based comparative genomic hybridization. *Lab Invest* **81**, 717-23 (2001).

181. Zhao, J. et al. Combined comparative genomic hybridization and genomic microarray for detection of gene amplifications in pulmonary artery intimal sarcomas and adrenocortical tumors. *Genes Chromosomes Cancer* **34**, 48-57 (2002).
182. Kononen, J. et al. Tissue microarrays for high-throughput molecular profiling of tumor specimens. *Nat Med* **4**, 844-7 (1998).
183. Shimizu, N., Shingaki, K., Kaneko-Sasaguri, Y., Hashizume, T. & Kanda, T. When, where and how the bridge breaks: anaphase bridge breakage plays a crucial role in gene amplification and HSR generation. *Exp Cell Res* **302**, 233-43 (2005).
184. Pan, Y. et al. 5q11, 8p11, and 10q22 are recurrent chromosomal breakpoints in prostate cancer cell lines. *Genes Chromosomes Cancer* **30**, 187-195 (2001).
185. Panagopoulos, I. et al. Fusion of the MORF and CBP genes in acute myeloid leukemia with the t(10;16)(q22;p13). *Hum Mol Genet* **10**, 395-404. (2001).
186. Snijders, A. M. et al. Assembly of microarrays for genome-wide measurement of DNA copy number. *Nat Genet* **29**, 263-4 (2001).
187. Bubendorf, L. et al. Survey of gene amplifications during prostate cancer progression by high-throughput fluorescence in situ hybridisation on tissue microarrays. *Cancer Res* **59**, 803-806 (1999).
188. El Gedaily, A. et al. Discovery of new DNA amplification loci in prostate cancer by comparative genomic hybridization. *Prostate* **46**, 184-90 (2001).
189. Wonderlin, W. F. & Strobl, J. S. Potassium channels, proliferation and G1 progression. *J Membr Biol* **154**, 91-107 (1996).
190. Mu, D. et al. Genomic amplification and oncogenic properties of the KCNK9 potassium channel gene. *Cancer Cell* **3**, 297-302 (2003).
191. Pei, L. et al. Oncogenic potential of TASK3 (Kcnk9) depends on K+ channel function. *Proc Natl Acad Sci U S A* **100**, 7803-7 (2003).
192. Pardo, L. A. et al. Oncogenic potential of EAG K(+) channels. *Embo J* **18**, 5540-7. (1999).
193. Basrai, D. et al. BK channel blockers inhibit potassium-induced proliferation of human astrocytoma cells. *Neuroreport* **13**, 403-7. (2002).
194. King, K. J., Nicholson, H. D. & Assinder, S. J. Effect of increasing ratio of estrogen: androgen on proliferation of normal human prostate stromal and epithelial cells, and the malignant cell line LNCaP. *Prostate* **66**, 105-14 (2006).
195. Parihar, A. S., Coghlan, M. J., Gopalakrishnan, M. & Shieh, C. C. Effects of intermediate-conductance Ca2+-activated K+ channel modulators on human prostate cancer cell proliferation. *Eur J Pharmacol* **471**, 157-64 (2003).
196. Pardo, L. A. Voltage-gated potassium channels in cell proliferation. *Physiology (Bethesda)* **19**, 285-92 (2004).
197. O'Grady S, M. & Lee, S. Y. Molecular diversity and function of voltage-gated (Kv) potassium channels in epithelial cells. *Int J Biochem Cell Biol* **37**, 1578-94 (2005).
198. Peres, A., Zippel, R. & Sturani, E. Serum induces the immediate opening of Ca2+-activated channels in quiescent human fibroblasts. *FEBS Lett* **241**, 164-8 (1988).
199. Wu, S. N. Large-conductance Ca2+- activated K+ channels:physiological role and pharmacology. *Curr Med Chem* **10**, 649-61 (2003).
200. Manche, L., Green, S. R., Schmedt, C. & Mathews, M. B. Interactions between double-stranded RNA regulators and the protein kinase DAI. *Mol Cell Biol* **12**, 5238-48 (1992).
201. Minks, M. A., West, D. K., Benvin, S. & Baglioni, C. Structural requirements of double-stranded RNA for the activation of 2',5'-oligo(A) polymerase and protein kinase of interferon-treated HeLa cells. *J Biol Chem* **254**, 10180-3 (1979).
202. Elbashir, S. M., Lendeckel, W. & Tuschl, T. RNA interference is mediated by 21- and 22-nucleotide RNAs. *Genes Dev* **15**, 188-200 (2001).

203. Cheadle, C. et al. Stability regulation of mRNA and the control of gene expression. *Ann N Y Acad Sci* **1058**, 196-204 (2005).
204. Dick, G. M., Rossow, C. F., Smirnov, S., Horowitz, B. & Sanders, K. M. Tamoxifen activates smooth muscle BK channels through the regulatory beta 1 subunit. *J Biol Chem* **276**, 34594-9. (2001).
205. Dick, G. M., Hunter, A. C. & Sanders, K. M. Ethylbromide tamoxifen, a membrane-impermeant antiestrogen, activates smooth muscle calcium-activated large-conductance potassium channels from the extracellular side. *Mol Pharmacol* **61**, 1105-13 (2002).
206. Duncan, R. K. Tamoxifen alters gating of the BK alpha subunit and mediates enhanced interactions with the avian beta subunit. *Biochem Pharmacol* **70**, 47-58 (2005).
207. Ho, S. M. Estrogens and anti-estrogens: key mediators of prostate carcinogenesis and new therapeutic candidates. *J Cell Biochem* **91**, 491-503 (2004).
208. Soronen, P. et al. Sex steroid hormone metabolism and prostate cancer. *J Steroid Biochem Mol Biol* **92**, 281-6 (2004).
209. Lau, K. M., LaSpina, M., Long, J. & Ho, S. M. Expression of estrogen receptor (ER)-alpha and ER-beta in normal and malignant prostatic epithelial cells: regulation by methylation and involvement in growth regulation. *Cancer Res* **60**, 3175-82 (2000).
210. Linja, M. J., Savinainen, K. J., Tammela, T. L., Isola, J. J. & Visakorpi, T. Expression of ERalpha and ERbeta in prostate cancer. *Prostate* **55**, 180-6 (2003).
211. Wang, Z. Roles of K+ channels in regulating tumour cell proliferation and apoptosis. *Pflugers Arch* **448**, 274-86 (2004).
212. Kunzelmann, K. Ion channels and cancer. *J Membr Biol* **205**, 159-73 (2005).
213. Wang, L., Reinach, P. & Lu, L. TNF-alpha promotes cell survival through stimulation of K+ channel and NFkappaB activity in corneal epithelial cells. *Exp Cell Res* **311**, 39-48 (2005).
214. Pedersen, S. F., Hoffmann, E. K. & Mills, J. W. The cytoskeleton and cell volume regulation. *Comp Biochem Physiol A Mol Integr Physiol* **130**, 385-99 (2001).
215. Roovers, K. & Assoian, R. K. Effects of rho kinase and actin stress fibers on sustained extracellular signal-regulated kinase activity and activation of G(1) phase cyclin-dependent kinases. *Mol Cell Biol* **23**, 4283-94 (2003).
216. Lang, F. et al. Ion channels in cell proliferation and apoptotic cell death. *J Membr Biol* **205**, 147-57 (2005).
217. Kaighn, M. E., Narayan, K. S., Ohnuki, Y., Lechner, J. F. & Jones, L. W. Establishment and characterization of a human prostatic carcinoma cell line (PC-3). *Invest Urol* **17**, 16-23 (1979).
218. Sobel, R. E. & Sadar, M. D. Cell lines used in prostate cancer research: a compendium of old and new lines-part 1. *J Urol* **173**, 342-59 (2005).
219. Horoszewicz, J. S. et al. The LNCaP cell line--a new model for studies on human prostatic carcinoma. *Prog Clin Biol Res* **37**, 115-32 (1980).
220. Horoszewicz, J. S. et al. LNCaP model of human prostatic carcinoma. *Cancer Res* **43**, 1809-18 (1983).
221. Karan, D. et al. Decreased androgen-responsive growth of human prostate cancer is associated with increased genetic alterations. *Clin Cancer Res* **7**, 3472-80 (2001).
222. Hayward, S. W. et al. Establishment and characterization of an immortalized but non-transformed human prostate epithelial cell line: BPH-1. *In Vitro Cell Dev Biol Anim* **31**, 14-24 (1995).
223. Sobel, R. E. & Sadar, M. D. Cell lines used in prostate cancer research: a compendium of old and new lines-part 2. *J Urol* **173**, 360-72 (2005).

224. Sambrook, J., Fritsch, E. F. & Maniatis, T. *Molecular Cloning: A Laboratory Manual* (Cold Spring Harbour Press, New York, 1989).

Michael Bloch
Mittlere Str. 67
CH-4056 Basel
Switzerland

Phone: +41796067180
e-mail: michaelbloch@gmx.ch

Michael Bloch - Curriculum Vitae:

*16.6.1976 Oxford (GB)

20.12.1995	Matura, Gymnasium in Oberwil (Switzerland)
1996-2001	Studies in 'Biology 2' (Molecular Biology, see below) at the University of Basel (Switzerland).
16.10.1997	1. Vordiplom' examination Biology 2, University of Basel.
15.10 1998	2. Vordiplom' examination Biology 2, University of Basel.
1999-2000	Diploma Thesis with specialisation in Microbiology: ‚Two colour in vivo fluorescence microscopy may provide valuable methods to study dynamic processes in cellular biology of the budding yeast Saccharomyces cerevisiae'. The project was supervised by Prof. Peter Philippsen.
3.4.2001	Diploma Biology 2, University of Basel.
2001-2006	PHD thesis at the University Basel with specialisation in biomedical research. Title: 'Amplification of KCNMA1: A Potential Therapeutic Target in Prostate Cancer?' under the guidance of Prof. L. Bubendorf, Institute of Pathology, University Hospital Basel. The Project was supervised by Prof. Dr.med. Christoph Moroni and Prof. Dr. Nancy Hynes
26.4.2006	Thesis defense PHD